Department of the Interior
U.S. Geological Survey

Field Guide to Neotectonics of the San Andreas Fault System, Santa Cruz Mountains, in Light of the 1989 Loma Prieta Earthquake

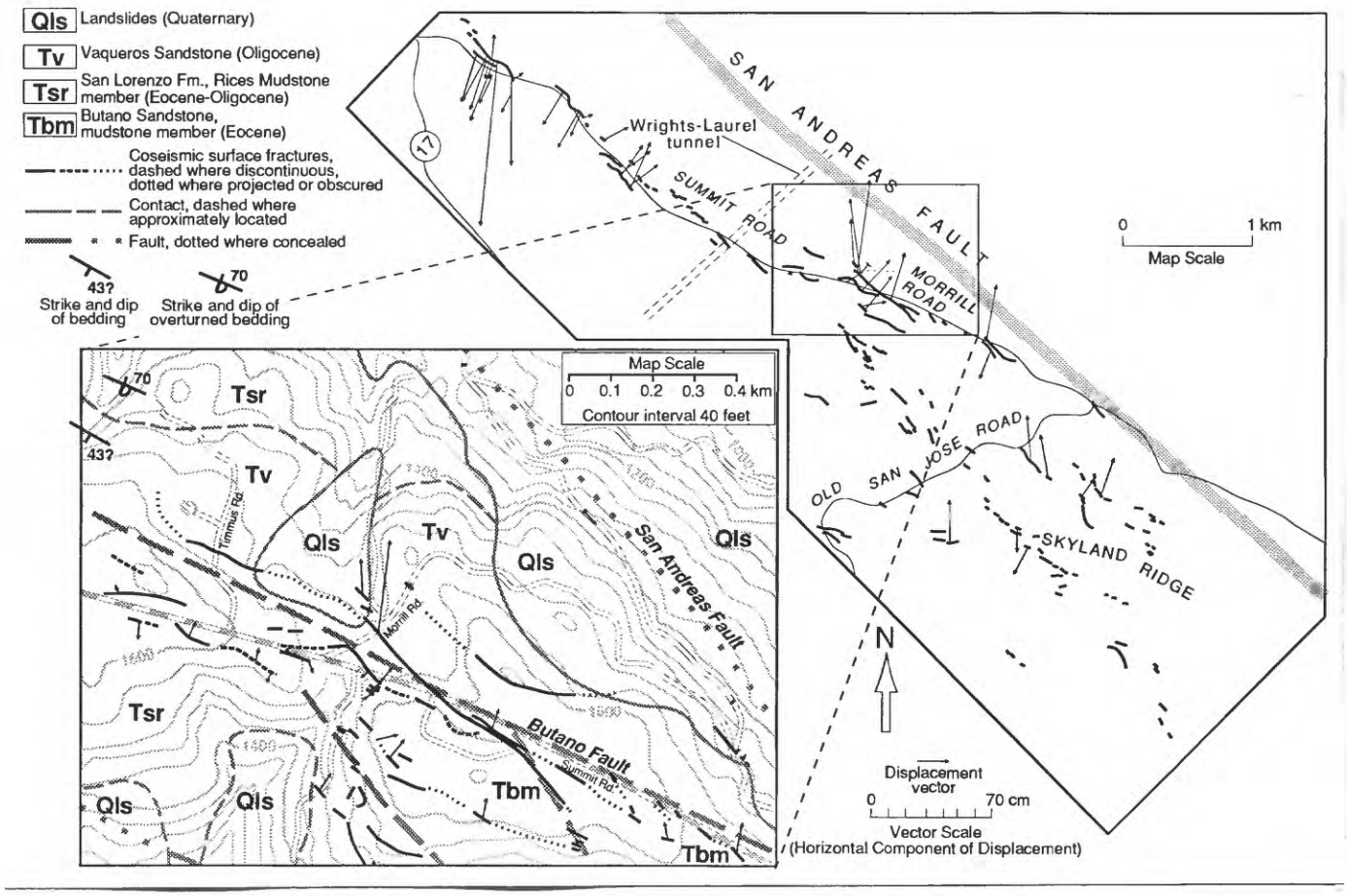

OPEN-FILE REPORT 90-274

Menlo Park, California

April 27, 1990

Department of the Interior
U.S. Geological Survey

Field Guide to Neotectonics of the San Andreas Fault System, Santa Cruz Mountains, in Light of the 1989 Loma Prieta Earthquake

David P. Schwartz and Daniel J. Ponti, editors
U. S. Geological Survey
Menlo Park, CA 94025

with contributions by:

Robert S. Anderson	*U.C. Santa Cruz, Santa Cruz, CA*
William R. Cotton	*William Cotton and Associates, Los Gatos, CA*
Kevin J. Coppersmith	*Geomatrix Consultants, San Francisco, CA*
Steven D. Ellen	*U. S. Geological Survey, Menlo Park, CA*
Edwin L. Harp	*U. S. Geological Survey, Menlo Park, CA*
Ralph A. Haugerud	*U. S. Geological Survey, Menlo Park, CA*
Robert J. McLaughlin	*U. S. Geological Survey, Menlo Park, CA*
Daniel J. Ponti	*U. S. Geological Survey, Menlo Park, CA*
Carol S. Prentice	*U. S. Geological Survey, Menlo Park, CA*
David P. Schwartz	*U. S. Geological Survey, Menlo Park, CA*
Gerald E. Weber	*U.C. Santa Cruz and Weber and Associates, Santa Cruz, CA*
Ray E. Wells	U. S. *Geological Survey, Menlo Park, CA*

OPEN-FILE REPORT 90-274

Menlo Park, California

April 27, 1990

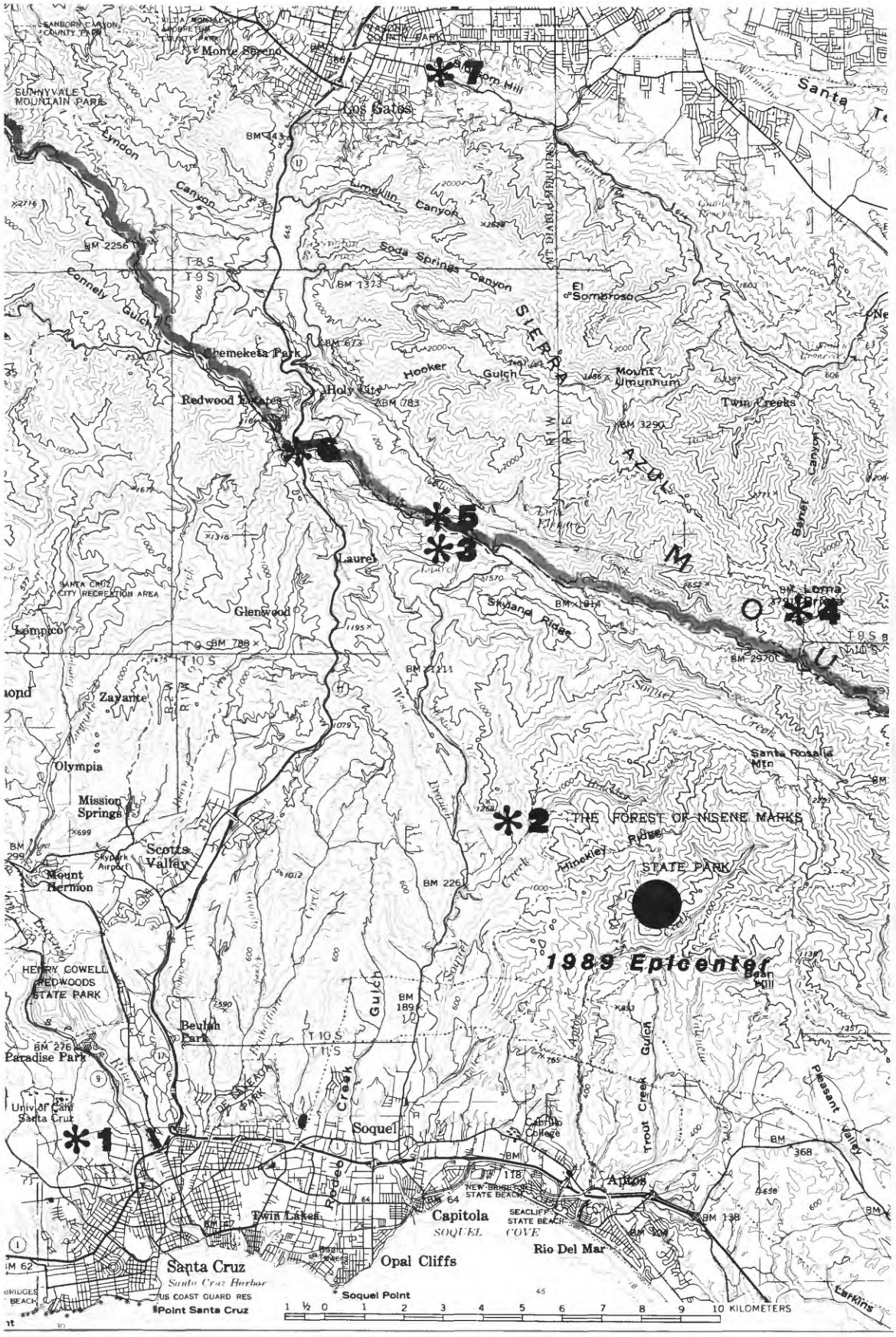

Map of field trip stops

ROAD LOG

Cumulative Miles	
0	Leave Dream Inn. Go north on Bay Street.
1.0	Cross Mission Street (Highway 1). Follow signs to UCSC campus and climb the hill past the entrance to the lower campus. Continue up this east side road past the Cowell farm buildings, past the intersection with Hagar Court/ Hagar Drive, and 0.6 miles further to a turnout on the right side of the road. Park here, at the overlook to northern Monterey Bay.
3.1	**STOP 1:** Marine Terrace deformation pattern: Its implications for repeat times of Loma Prieta earthquakes and for the long-term evaluation of the Santa Cruz Mountains.
5.2	Retrace route and turn left on Mission.
6.8	Cross San Lorenzo River. Liquefaction related ground failure was widespread from Santa Cruz to near Salinas in areas underlain by late-Holocene unconsolidated deposits of the San Lorenzo, Pajaro, and Salinas Rivers. Lateral spreads caused displacements ranging from a few millimeters to about 2 m. The most widespread damage was to levees of the Pajaro and San Lorenzo Rivers, which suffered cracking due to differential settlements and small transitional displacements at many locations of liquefaction.
10.7	Exit freeway to Capitola- Soquel. Go left on Porter Street to Soquel.
11.1	Cross Soquel Drive. Porter Street becomes Soquel-San Jose Road.
11.4	Road is on Holocene terrace of Soquel Creek.
13.7	Roadcuts expose south-dipping beds of marine sandstones and siltstones of the Pliocene Purisima Formation. From here to mile 21.9, all outcrops are of the Purisima Formation.
15.3	Cross bridge and turn right on Olive Springs Road. The epicenter of the 1989 earthquake is located 5 km due east of here.
16.6	Quarry scales on left.
16.9	Quarry gate.
17.1	**STOP 2:** The Zayante-Vergeles Fault Zone
19	Retrace route and make right on Soquel-San Jose Road.
19.8	Road follows Hester Creek on the right.
21.9	Road crosses into Eocene conglomerates of the Butano Sandstone.
22.9	Road crosses trace of Zayante fault.
24.4	Road crosses into Oligocene-Miocene Vaqueros Sandstone.
25.8	Make left on the Morrell Cutoff Road. Note damaged house at intersection.
27	**STOP 3:** The Morrell Cutoff Landslide: An example of a Deep-Seated Rotational Slump Triggered by the October 17, 1989, Earthquake
27.6	Intersection with Summit Road. Turn right.
28	Loma Prieta School on left. The Loma Prieta elementary school was closed in the spring of 1989 because geologic studies mandated by the California Alquist-Priolo Special Studies Zones Act found that Holocene-active faults associated with the San Andreas fault system passed underneath several of the school buildings. At least one of the faults identified in the exploratory trenches experienced displacement during the Loma Prieta earthquake. The zone of distress extended under two school buildings and caused considerable structural damage. Other earthquake-generated cracks were noted in the asphalt school yard and to a lesser degree in the natural ground. These cracks, however, did not display any measurable slip and could not be correlated to any bedding planes or fault surfaces that were logged in the

Cumulative Miles	
	exploratory trenches. It was apparent from the engineering geologic investigation performed by Rogers E. Johnson and Associates that several of the faults that passed through the school site were zones of repeated faulting and that in an event like the 1989 Loma Prieta earthquake, damaging ground rupture could recur. To our knowledge, this is the only case where a school site was abandoned because of a high potential for surface faulting, which then actually occurred.
28.5	Burrell School (now abandoned) on right. We are now entering the linear, geomorphically young, rift zone of the main trace of the San Andreas fault. Investigators were at this location in 1906 but did not report right-lateral offsets.
29	Intersection with Old San Jose-Soquel Road. Continue along Summit Road.
31.1	Well-developed rift topography on right.
31.2	Burrell guard station.
31.5	Sag pond on right.
31.7	Stop sign. Bear left onto Mt. Bache Road. Directly to the southeast the San Andreas fault drops into the deep ravines of Asbury Gulch and Soquel Creek. From here to Loma Prieta Peak, Mt. Bache crosses a sequence of northwest striking steeply northeast- to southwest-dipping Eocene (?) to Lower Miocene marine shales, sandstones, and mudstones and Upper Jurassic to Upper Cretaceous sandstones, shales, and conglomerates. These are displaced by a series of sub-vertical to steeply southwest dipping reverse faults.
34.9	Pavement ends.
35.6	Go left at intersection through green gate.
37.3	**STOP 4:** Sargent Fault Zone at Loma Prieta. Loma Prieta is the highest peak in the Santa Cruz Mountains at 3791 feet. Geodetic measurements indicate that the peak subsided about 14 cm as a result of the 1989 earthquake. The topographic saddle and uphill facing notches that can be seen on the west side of the peak occur along the steeply southwest dipping trace of the Sargent fault zone. Also visible from the peak is the San Andreas Rift Valley, the Santa Clara Valley and the Calaveras fault, Santa Cruz, and the Summit Road region.
42.9	Retrace route, make right onto Summit Road.
47	Right turn onto Morrill Road.
47.1	**STOP 5:** Surface Fractures Associated with the 1906 and 1989 Earthquakes.
47.2	Retrace route, turn right onto Summit Road.
47.5	Del Monte Road. Note closed depression. Closed depressions and linear breaks in slope are typical of the surface geomorphology of the Summit Road ridge area. Many of these features were previously mapped by Sarna-Wojcicki and others (1975) and interpreted as part of a complex zone of faulting associated with the San Andreas fault.
48.3	Pony corral on left. The corral sits in a pronounced northwest-trending, elongate ridge-top depression that measures approximately 500 m long and 200 m wide and has a topographic closure of nearly 3 m. Two extensional ground fractures developed along the southwestern and northeastern flanks of the depression during the earthquake. Ground cracks can still be observed on the south end of the southwest rupture. The depression has resulted from repeated displacements similar to those observed in 1989.
48.4	Road crosses trace of Butano fault. The fault separates Vaqueros Sandstone on the northeast from San Lorenzo Formation and Butano Sandstone on the southwest.
49.2	Note large left-lateral offset in yellow center stripe of road. This offset is part of the Tranbarger ground failure. As we slow down we can observe the now graded and modified Tranbarger crack in front of the pink house. This locality was a media mecca in the early

Cumulative Miles	
	days following the 1989 earthquake. Geologic mapping has documented a 335 m long by 76 m wide zone of scarps, and fissures that crosses the axis of Summit Road ridge. Extensional ground fissures up to 1 m wide and 2 m deep, compressional mole tracks up to 15 m long, and a pronounced left-lateral displacement of Summit Road of up to 90 cm horizontal and 40 cm vertical, make this feature one of the largest and certainly most highly publicized of the Loma Prieta earthquake. The Tranbarger fissure was pictured in dozens of local and national newspapers and magazines immediately following the October 17, 1989 event.
	Along much of its length, the Tranbarger fissure is associated with geomorphic features such as topographic furrows and sidehill benches that are the result of repeated episodes of slip. Geometric analysis of the fissure where it crosses a drainage swale near its western end, indicates that the fissure strikes N40°W and dips 59°SW. This attitude conforms with the regional bedrock attitudes of the Vaqueros Sandstone (generally N40-65°W d50-60°S), and suggests that the fracture is related to slip along bedding.
53.1	Intersection with Highway 17. Go right (toward Santa Cruz), cross overpass, and continue ahead up hill to left.
53.3	Junction with Mtn. Charlie Road and overlook above Patchen Pass.
	STOP 6: Highway 17 Deformation.
	Leave overlook, retrace route across overpass.
53.6	Turn right onto Highway 17 towards San Jose.
56.6	Highway crosses the main trace of San Andreas fault. Lexington Reservoir, the approximate northwest end of the deep 1989 rupture zone, is on the right.
56.9	Old Santa Cruz Highway on right.
59.7	Exit left to Los Gatos.
60.4	Take exit for East Los Gatos. Go east on Saratoga Avenue, through light at Los Gatos Motor Inn.
60.8	Turn left onto Los Gatos Boulevard. Continue through light at Kennedy Road, another light, and right at Shannon Road.
61.6	Turn right onto Blossom Hill Road. Continue through light on Cherry Blossom Lane.
62.7	Turn left onto Camino del Cerro. Go two blocks, turn right on Winchester, go two blocks, turn right on Dover, go one block and park at corner.
	STOP 7. Coseismic Ground Deformation Along the Northeast Margin of the Santa Cruz Mountains.
	Turn right on Blossom Glen Way, go one block and turn left onto Camino del Cerro, turn right on Blossom Hill Road, turn left at Los Gatos Boulevard, turn right at Saratoga Avenue, get on to Highway 17, and return to Santa Cruz.

Introduction

David P. Schwartz, USGS

The Loma Prieta earthquake has been described as an anticipated event (USGS Staff, 1990), and in many respects it was. But there were also some aspects that, while understandable in retrospect, would probably not have been anticipated prior to this earthquake. Perhaps the most obvious "surprise" was the lack of throughgoing coseismic surface faulting along the main trace of the San Andreas fault. In hindsight this was clearly a function of the greater than typical depth (18 km) of this earthquake; had the same size event nucleated at the more common depth of 10-12 km there undoubtedly would have been surface faulting. Regardless of this, the absence of surface faulting from an M7 San Andreas event raises some important questions about paleoseismology and our ability to recognize past earthquakes in the geologic record, characteristic earthquakes, and fault segmentation. These have important implications for defining the behavior of faults and for quantifying input parameters for seismic design and hazard analysis, particularly maximum earthquakes for ground motions, earthquake recurrence intervals, and long-term probabilistic forecasting of where and when earthquakes are likely to occur along a fault.

The 1989 earthquake occurred along a segment of the San Andreas fault zone that passes through a long double restraining (left) bend. Deformation within this bend occurs across a broad zone of fault-normal compression extending from the coast to the Santa Clara Valley; it is topographically and geomorphically expressed by the high elevations of the Santa Cruz Mountains and uplifted coastal terraces. The deformation is accommodated as folding and by a series of oblique and reverse-slip faults that include the Zayante, San Andreas, Sargent, Berrocal, and Shannon faults as well as a variety of less extensive structures. Seismologic, geodetic, and geologic observations from the Loma Prieta event provide insights into the dynamics and kinematics of restraining bends. They also raise intriguing questions about spatial and temporal strain partitioning within the bend, and the seismogenic potential of individual structural elements other than the San Andreas fault.

The field trip provides an opportunity to look at the ways the 1989 earthquake has affected the understanding of the neotectonic development of the Santa Cruz Mountains and, conversely, how knowledge of the structure and geologic history of the area affects our interpretation of the Loma Prieta event and the earthquake history of the San Andreas fault. At Stop 1, University of California Santa Cruz campus, we will observe uplifted marine terraces and discuss their development in light of geodetically modeled 1989 uplift. Stop 2 at Olive Spring Quarry presents a discussion of the Zayante fault, a major structure in the restraining bend that is associated with pre-1989 seismicity and may be a source of some 1989 aftershocks. Stop 3 gives us a chance to walk along a large landslide that occurred near Summit Road on October 17. Stop 4 is at the peak of Loma Prieta, where we will observe the geometry and geomorphic expression of the Sargent fault and discuss its history and the possible role that it played in the 1989 earthquake. This stop also provides a magnificent overview (weather permitting) of the entire restraining bend. At Stop 5, Morrill Road, we will look at surface cracks from 1989 that were also active in 1906, discuss what is known of 1906 faulting and ground cracking in the Santa Cruz Mountains, and discuss the extent and possible mechanisms of formation of the 1989 Summit Road-Skyland Ridge ground cracks. Stop 6, at Summit Road and Highway 17, affords the opportunity to observe some of the structural and lithologic relationships that may control the style of slip and location of many of the 1989 ground cracks. At Stop 7, Los Gatos, we will observe deformation of curbs that occurs in proximity to the Shannon fault and may represent coseismic slip along a range-front reverse fault on the northeast side of the Santa Cruz Mountains.

We hope the field trip provides a stimulating forum for exchanging ideas, interpretations, and observations about the Loma Prieta earthquake and leads to an increased appreciation of the complex geology, structure, and geomorphic setting of the epicentral region.

Stop 1. Marine terrace deformation pattern: Its implications for repeat times of Loma Prieta earthquakes and for the long term evolution of the Santa Cruz mountains

Gerald E. Weber, UCSC and Weber Associates
and Robert S. Anderson, UCSC

The view: culture and topography

The view is east and south. We stand on the edge of the San Lorenzo River valley, looking down from a topographic high that stretches some 10 km north, called Ben Lomond Mountain (Figure 1.1). The entirety of Monterey Bay is visible, into which the San Lorenzo, the Pajaro, the Salinas, and the Carmel Rivers flow. Cultural features of note are the towns of Santa Cruz to the right, Capitola, Soquel and Aptos in the middle foreground, Watsonville further along the Bay, the Moss Landing power plant in mid-Bay, and in the distance the town of Monterey, at the other end of the bay.

The dominant topographic feature of the San Francisco peninsula is the Santa Cruz Mountains. The San Andreas fault crosses the Santa Cruz Mountains approximately in their middle, dividing the range into roughly equal northern and southern ranges. This crossing occurs at the summit ridge we will visit later in the day, roughly where Highway 17 crosses the range. The topographic maxima of the range lie close to the bend in the San Andreas (the Santa Cruz bend), and the main crest of each range lies within about 2-3 km of the trace of the San Andreas throughout its length. The highest point in the southern range is Loma Prieta (el. 3791 ft.); the highest point

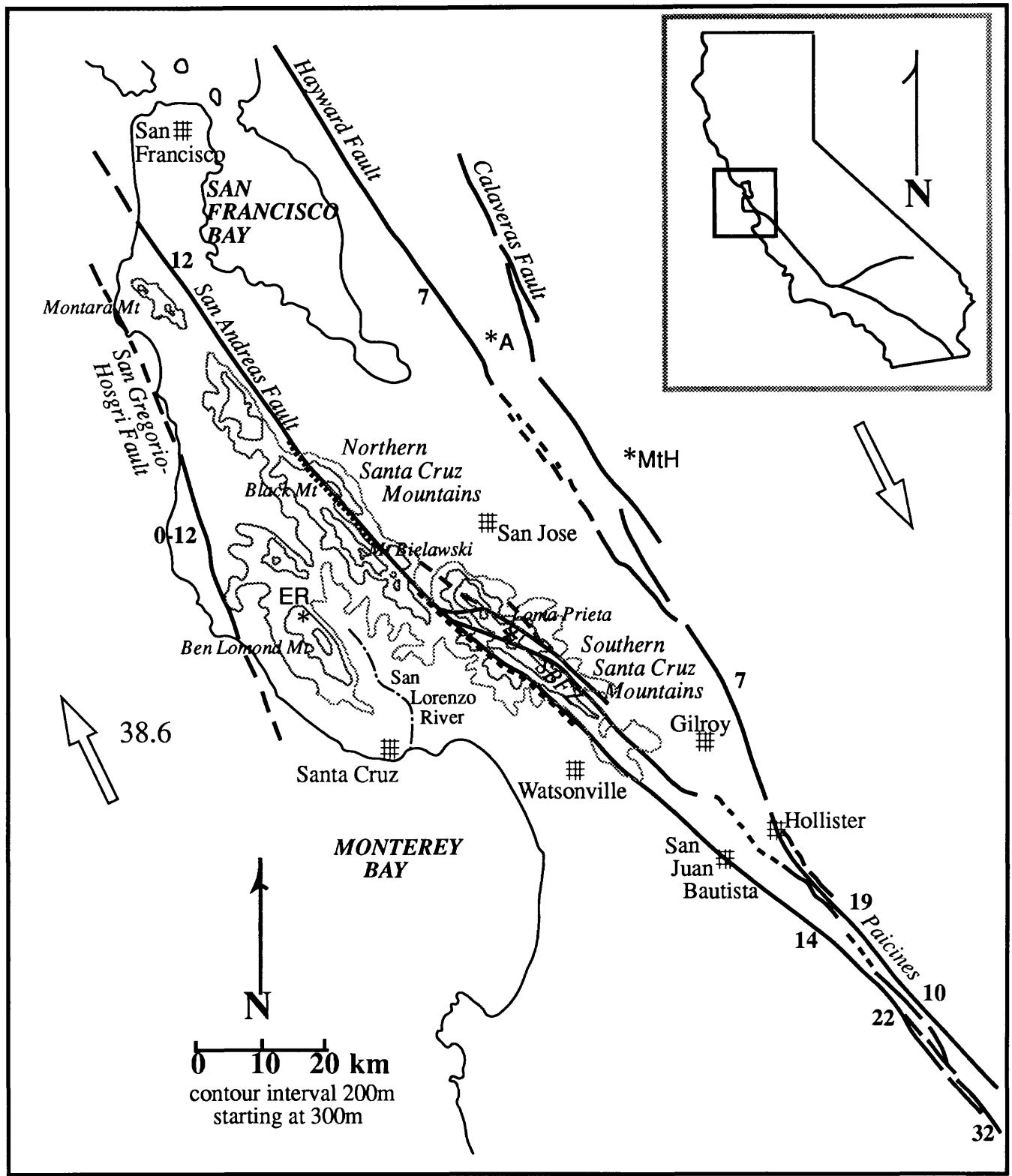

Figure 1.1 Map of the Santa Cruz Mountains surrounding the slight bend in the San Andreas in which the recent October 17, 1989 earthquake nucleated. Index maps shows the San Andreas as it passes through California. Note the broad bend in the Monterey Bay region separating very straight reaches of the fault. This bend is accomplished by a smaller 3 km amplitude, 30 km long bend to the northeast of Santa Cruz (the Santa Cruz bend, long dashed lines), and a second bend associated with Black Mountain further north (the Black Mountain bend, short dashed lines). Topographic contours are shown at 200 m intervals from 300 m up. The San Andreas crosses between the ranges in the Santa Cruz bend. The mountains to the northwest of the bend are to the west of the fault, those to the southeast of the bend to the east of the fault. The tallest portion of each segment of the range (Mt. Bielawski and Loma Prieta in the north and south, respectively) is closest to the bend. The crests (and the associated cross-sectional area of the ranges) decline with distance from the bend. Other topography in the region is not shown.

in the northern range is Mt Bielawski (el. 3231 ft.), best viewed from San Jose and the Bay area (and near where Highway 9 crosses the range).

Loma Prieta ("dark peak") graces the summit of the southern Santa Cruz Mountains, forming the skyline on the left. Further in the distance is a set of ranges and intervening valleys, from right to left starting at the distant tip of Monterey Bay, the Santa Lucia range, Carmel Valley, Sierra de Salinas, and the Salinas Valley . The Gabilan Range ,forming the eastern side of the Salinas Valley, is hidden behind the southern extension of the Santa Cruz Mountains. The San Lorenzo River Valley seen below is the major drainage in the Santa Cruz area, with headwaters in the Santa Cruz mountains. Major tributaries extend behind Ben Lomond mountain, and form the valley in which the towns of Felton, Ben Lomond and Boulder Creek sit.

The geology

The geology of the area is summarized in several recent publications (Clarke, 1981; Brabb, 1989; Aydin and Page, 1984). We are standing on a fragment of the Salinian block, comprised here of limestones and metasedimentary rocks of Paleozoic and Mesozoic age intruded by Cretaceous quartz diorite. It is the limestone that controls the sinkhole topography in nearby meadows, and throughout the campus. This limestone was mined on this land in the early 20th century, in several large quarries, and calcined in the kilns you drove past among the farm buildings at the base of campus. Another such chunk of Salinian basement dominated by Cretaceous granite forms the topographic high of the Santa Lucia Range in the distance.

The trace of the San Andreas is visible as it abuts the base of the southern Santa Cruz Mountains further south. Although this is difficult to see at this range, we note that the trace is nowhere near as knife-sharp as it is in the Carrizo Plain, for instance. Numerous landslides obscure the trace of the fault.

The lowlands in the foreground sandwiched between the ocean and Loma Prieta are composed of significantly more easily eroded late Cenozoic sedimentary rocks. These comprise a generally shoaling sequence of marine rocks. In the Watsonville area the geology is dominated by the more recent Aromas Formation, which is composed chiefly of eolian sands. The hummocky topography visible in the Watsonville area owes its existence to this stabilized dune field. The area of the epicenter is in the unpopulated forested region inland of the largest indentation in the coastline, the Forest of Nisene Marks.

Between here and Watsonville, however, the lowlying topography is dominated by a series of large flat-topped steps, the lowest of these being the flattest, least vegetated, and most extensive, the older ones being more and more deeply incised. Three major steps are plainly visible. These are uplifted or emergent marine terraces. They continue in even more impressive fashion further to the north (along the 'north coast'), there comprising a series of up to 6 identifiable terrace remnants.

The view below shows clearly how most of the settlement in the Santa Cruz area utilizes the lowermost of these terrace surfaces. Highway 1 as it heads south to Watsonville follows this terrace. This is a fortunate circumstance, as the enhancement of seismic shaking on these platforms, with their thin sequence of terrace deposits, resulted in only minor damage to residences and businesses even this close to the epicenter.

We would like to talk first about the process of marine terrace formation in general, and about what is known of the terrace ages in the Santa Cruz area, as a prelude to discussing the relevance of these terraces to our understanding of the Loma Prieta earthquake, in particular to the calculation of the repeat times of Loma Prieta type events.

Part A. Marine terraces and dating of the Santa Cruz terrace sequence

Gerald E. Weber, UCSC and Weber Associates.

Marine terraces are wave-cut benches characteristic of exposed, tectonically active coastlines. They are old ocean floors formed by wave erosion in the surf zone that have subsequently been stranded by a combination of tectonic uplift and sea level drop. They typically occur as narrow, bench-like steps in the coastal topography within a few hundred meters of the present sea level. Each terrace consists of a gently sloping erosional (or abrasional, or wavecut) platform backed by a near-vertical sea cliff at its inland edge. The intersection of the sea cliff and the wavecut platform is the shoreline angle (strandline, inner edge, back edge), which closely approximates the mean sea level at the time it was formed, and is virtually horizontal (see Weber [1990] for a more lengthy description).

The wavecut platform is commonly covered by a regressive sequence of shallow marine deposits, overlain by subaerial fluvial and colluvial deposits and windblown sand (Figure 1.2). The veneer of near-shore marine deposits is often characterized by a thin cobble and boulder lag directly overlying the wavecut platform, that may contain fossil shells. Terrace deposits are thickest along the back or inner edge of the terrace and thin progressively toward the seaward or distal edge. The wavecut cliff itself degrades by weathering and subsequent transport of particles in largely diffusive processes. This rounds off the cliff and creates the colluvial apron at its base that buries the wavecut platform and its marine cover. The paleo-cliff is also incised by drainages seeking to establish grade with the more recent lower sea level.

Clearly, these horizontal inner edges established in the past and preserved by the long term uplift of the land relative to the sea comprise potentially useful paleo-horizontal and paleo-mean sea level datums. We must, however, know three things about a particular marine terrace in order to make them useful as long term recorders of uplift patterns: (1) the elevation of the inner edges of the wavecut platforms, (2) the age of the wavecut platform, and (3) the elevation with respect to modern sea level at which the wavecut platform was formed (the formation elevation).

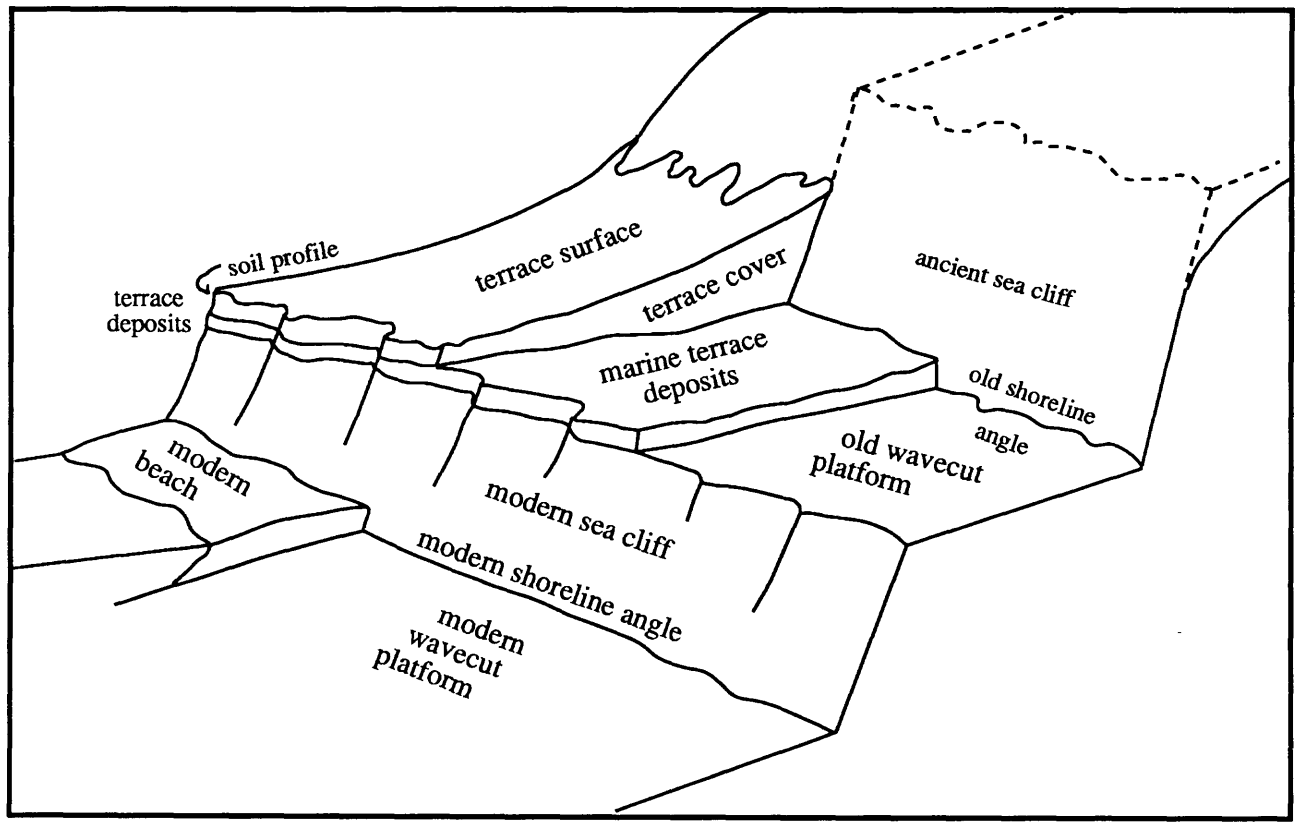

Figure 1.2 Schematic diagram showing marine terrace features.

Old shoreline angle elevations

Only rarely has a stream incised a terrace deeply enough to expose the old shoreline angle. In the absence of a direct measure of its elevation, such information may be obtained by either shallow refraction seismic techniques (e.g., Bradley and Griggs, 1976), or by a mapping technique that draws heavily upon an analogy with the morphology of modern wavecut platforms reported by Bradley (1958) and Bradley and Griggs (1976). The wavecut platform is projected inland (Figure 1.3), and the elevation of the old shoreline angle is found by making the following assumptions, moving from offshore toward the coast: (1) the outer portion of the wavecut platform (to within about 600 m of the old shoreline) slopes 0.5° seaward; (2) the inner portion slopes 1° seaward ; and (3) the paleo sea cliff lies near the inflection point on the face of the erosionally modified paleo sea cliff.

Obviously, this technique is fraught with difficulties, but it is the best we can do in the absence of further elevation control on the wavecut platform itself. Clearly, any additional information gathered from well logs or from shallow seismic surveys aids in constraining the elevation of the old shoreline angle.

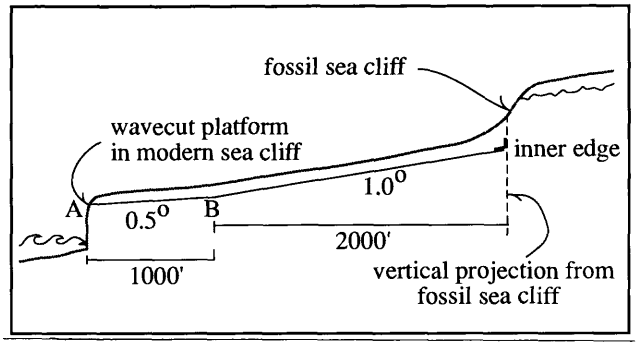

Figure 1.3 Diagram showing technique used to calculate shoreline angle (inner edge) elevations. If elevation of wavecut platform in modern sea cliff and horizontal distance to fossil sea cliff are known, elevation of shoreline angle can be calculated. For example: elevation at point B = 39' (1000' x tan [0.5°] = 9'; therefore, inner edge elevation = 74' (2000' x tan [1.0°] = 35').

Terrace ages and formation elevations

Determination of terrace ages may be accomplished using either absolute or relative age techniques. (See Lajoie [1986] for a more extensive discussion of terrace dating techniques.) The direct methods (and therefore presumably the most reliable) involve dating fossil shells found on at the wavecut platform (yielding a maximum age), or by dating soils developed on the terrace surface (a minimum age). Given the general thickness of the terrace cover and poor exposure of wavecut platforms, fossils are generally scarce. Absolute ages may be obtained from shells through U-series dating, or if young enough, ^{14}C techniques. However, U-series dating is of questionable reliability when used on molluscs, and is best used on corals, effectively restricting its use to tropical latitudes.

The relative dating techniques include (1) amino acid stereochemistry studies of fossil shell material, (2) faunal associations indicative of relative water temperature, (3) geomorphic modelling of the processes modifying the paleo sea cliffs (Hanks and others, 1984), and (4) correlation techniques based upon the assumption that the terraces reflect global (eustatic) highstands of the sea level. The first two techniques obviously require shell material. The second, although quite handy in correlation of terraces along a coastline, does not typically provide sufficient resolution to allow determination of an absolute age.

Most marine terrace ages are therefore determined by using the paleo-sea level curve obtained by subtracting tectonic uplift from the well-dated emergent coral terrace sequence on the Huon Peninsula in Papua, New Guinea (Figure 1.4: see Chappell, 1983; Lajoie, 1986). The sea-level highstands on this curve are assumed to be the formation elevations of the terraces in any sequence. The sea level highstands are associated with interglacial periods and therefore have odd isotope stage numbers; the sea level low stands, which correspond to global glaciations, are not recorded by emergent terraces, and have even isotope stage numbers. The simple graphical technique is illustrated in Figure 1.4. The shoreline angle elevations are plotted on the vertical axis, and lines are drawn between the shoreline angle elevations and sea-level highstands. If the uplift rate is constant, these lines will be parallel.

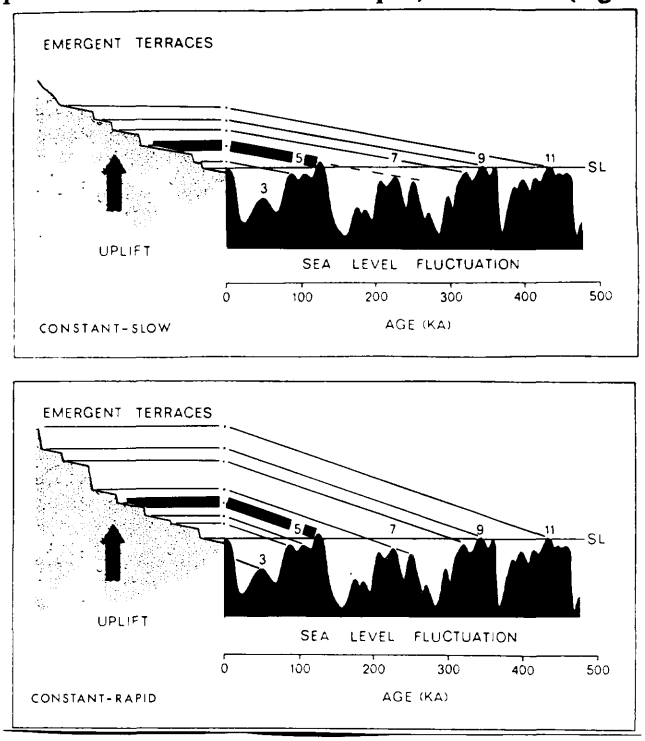

Figure 1.4 Age assignment of marine terraces based on global sea-level curves and a constant uplift model (see text for discussion).

The Santa Cruz terraces

Assessment of the Santa Cruz terraces began with Rode (1930), and has been followed by an increasing number of workers as new techniques have emerged (see Bradley 1957, 1958; Bradley and Griggs 1976; Hanks and others, 1984; Lajoie, 1986; Weber, Lajoie and Griggs, 1979; and Weber, 1990a,b). Most of the effort has been spent on the sequences along the north coast. These are the best exposed terraces, and their interpretation is important in the assessment of the slip on the San Gregorio fault system (Weber, 1990b). The sole source for detailed shoreline angle elevations along the coast sought of Santa Cruz is the work of Alexander (1953).

The naming of the local terrace sequence, and the latest interpretation of the terrace ages is shown in Table 1 (from Weber,1990b; Anderson,1990). Only two absolute ages have been obtained from the Santa Cruz terrace sequence (see Weber 1990b for discussion), both from shell material found on the two wavecut platforms (isotope stages 5a [84 ky] and 5c [105 ka]), buried by the terrace cover on the Santa Cruz terrace forming the foundation for the majority of the population in the town of Santa Cruz (Figure 1.5). This surface corresponds to the first terrace of Alexander (1953) south of Santa Cruz.

The road from Santa Cruz up to the view point (Stop 1) climbs from this Santa Cruz terrace surface up through a minor incision in the associated, now erosionally modified wavecut cliff, onto the older (isotope stage 7a [212 ka]) "Western terrace" surface. This latter surface corresponds to the "third terrace" of Alexander (1953). The intervening isotope stage 5e highstand (the highest sea level in the last several hundred thousand years) is somewhat surprisingly only represented by a short segment called the Cement terrace north of the town of Davenport, and by Alexander's "second terrace" south of Santa Cruz.

Higher terraces are found to the north of Santa Cruz in decreasing degrees of preservation. These are the Wilder (330 ka, isotope stage 9a), the Blackrock (490 ka, stage 13), and the Quarry (630 ka, stage 15) (see Hanks and others, 1984; Lajoie, 1986 for further discussion of these ages).

TABLE 1.

Terrace Name	Age (ky) (Bull, 1986)	Age(ky)(this report)	Isotope Stage	Formation Elevation (m)
Santa Cruz	103	84, 105	5a, 5c	x,-9
Cement	120	124	5e	+6
Western	214	212	7a	-7
Wilder	320	330	9a	+4
Black Rock		490	13	0?

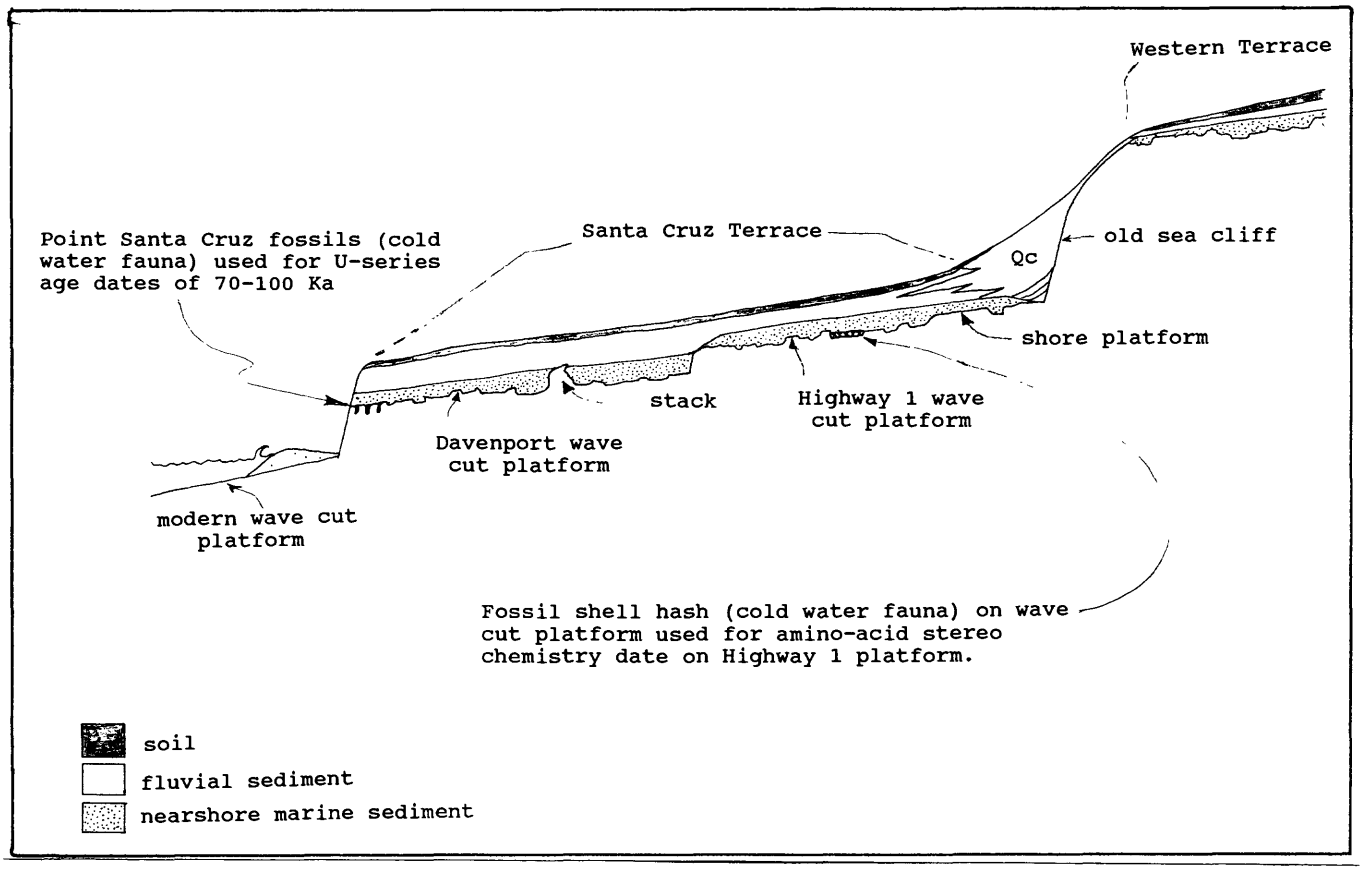

Figure 1.5 Cross-section showing Santa Cruz terrace sequence.

Part B. Reflection of repeated Loma Prieta uplift events in pattern of marine terrace elevations south of Santa Cruz,with implications for repeat times of Loma Prieta events,and for the evolution of the Santa Cruz mountains

Robert S. Anderson, UCSC

Heretofore, no general hypothesis has been advanced for the cause of the emergence of the terraces along the Santa Cruz coast. Figure 1.6 shows the elevations of all old shoreline angles along this reach of coast. Clearly, the elevation of any particular shoreline angle is not constant along the coast, but rather shows two prominent peaks, the most obvious to the south of Santa Cruz, centered about Aptos, the other the Greyhound Rock Arch noted by Bradley and Griggs (1976) 20 km to the north, which they attributed to domical uplift of the Ben Lomond mountain massif.

I have plotted the pattern of expected uplift due to the Loma Prieta event along the same transect of coastline on the same graph for comparison (Many thanks to Luca Valensise for providing the original plot of this back in November 1989; see also McNally and others (1989) and Plafker and Galloway (1989). It is the general correspondence of these curves that prompted the notion that the terraces owe their elevation to repeated seismic events. Not surprisingly, the terrace elevations are greatest along the coast closest to the epicenter of the earthquake giving rise to the uplift (Figure 1.7). The patterns of expected Loma Prieta uplift and of total uplift (present elevation less formation elevation) are plotted in Figure 1.6, this time normalized with respect to their maxima, the elevation (expected uplift) at Aptos. The correspondence in the area south of Santa Cruz is now even more striking, implying strongly a genetic tie.

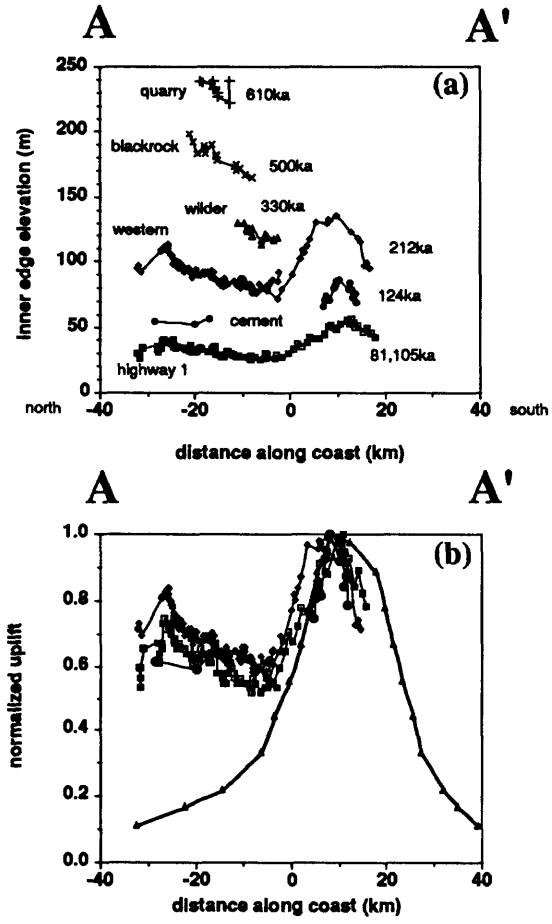

Figure 1.6 (a) Terrace elevations through the study area (section A-A'; see Figure 1.7) from published data (see text). All elevations taken at the back edge of the wavecut platform (refs: Bradley and Griggs (1976) for Santa Cruz north; Alexander (1953) for Santa Cruz south). The terraces all reach a peak elevation in the region of Aptos, roughly 8 km south of the mouth of the San Lorenzo River, and display a second maximum well to the north, representing what Bradley and Griggs (1976) dubbed the Greyhound Rock Arch. (b) Patterns of total uplift at the terrace back edges (difference between present elevations (Figure 1.6a) and formation elevations (Table 1), and Loma Prieta uplift (Figure 1.7), each normalized with respect to its maximum value to facilitate comparison of the patterns. That the patterns overlay so neatly in the region south of Santa Cruz implies that these normalization scales may be used to assess the total number of events required to create the terraces along this reach of the coast. Given the terrace ages from Table 1, recurrence times may then be calculated. Divergence of the patterns to the north implies the repeated action of other uplift events.

If this is true, then the number of events needed to raise a particular platform at a specific site to its present elevation from its initial "formation elevation" may be estimated by dividing the total uplift at that site by the local uplift per seismic event (Figure 1.7). The repeat time of these seismic events is then obtained by dividing the total age of the platform by the estimated number of events. The repeat times so estimated are of the order of 500-700 years.

These calculations require several assumptions. There is obviously error in the elevation of the inner edges, as these (especially along this reach of coast) are buried beneath terrace deposits at the base of the old degraded wavecut cliffs. We assume no other event is causing uplift of the terraces. We ignore the slip of the plate relative to the uplift pattern since the terrace formed (this is minor, however, as the product of slip rates of 12 mm/yr with 300,000 yrs terrace ages result in shifts of less than 1 km, which is very small relative to the scale of the uplift pattern— roughly 40-50 km). We ignore post-seismic deformation associated with relaxation of the newly imposed topographic load. The Loma Prieta event is assumed to be characteristic in the sense that it repeats the same pattern of slip (Schwartz and Coppersmith, 1984) and hence of vertical displacement, each time, and the uplift pattern associated with the recent earthquake is only poorly constrained by data at present. Nonetheless, although the magnitude of the uplift pattern will likely change somewhat as we learn more about the deformation from geodetic measurements now in progress, which will in turn alter the recurrence time estimates (downward for less uplift than presently modeled; upward for more observed uplift), the conclusion that the pattern of terrace elevations, and indeed the uplift of the terraces as a whole, results from repeated Loma Prieta events, remains robust.

Elsewhere I have argued that a longer term manifestation of repeated Loma Prieta-type seismic events is the formation of the northern Santa Cruz mountains on the Pacific Plate to the north of the bend in the San Andreas (Anderson, 1990a,b).

There are two major issues raised by the above hypotheses. First, inspection of Figures 1.6 and 1.7 reveals that only the southern half of the terrace elevation pattern may be explained by Loma Prieta event repetition. Some other event or combination of events must be responsible for the generation of high elevations along the north coast, and for the occurrence of the Greyhound Rock Arch. Two options exist: seismic activity along the San Gregorio Fault system with associated vertical displacement (Weber, 1990b), which has clearly horizontally displaced portions of these terraces even further to the north; and seismic activity on the San Andreas further north, perhaps associated with the Black Mountain restraining bend (Nishenko and Williams, 1985; Scholz, 1985). The increased offshore tilt of the marine terraces with age (at roughly 0.5°/Ma, Bradley and Griggs, 1976) seems to support an uplift maximum to the east of the terraces, which implies the latter scenario.

Second, while the first order features of the northern Santa Cruz Mountains topography may be explained by repeated Loma Prieta events, the southern Santa Cruz Mountains cannot. In particular, geodetic evidence collected by the USGS

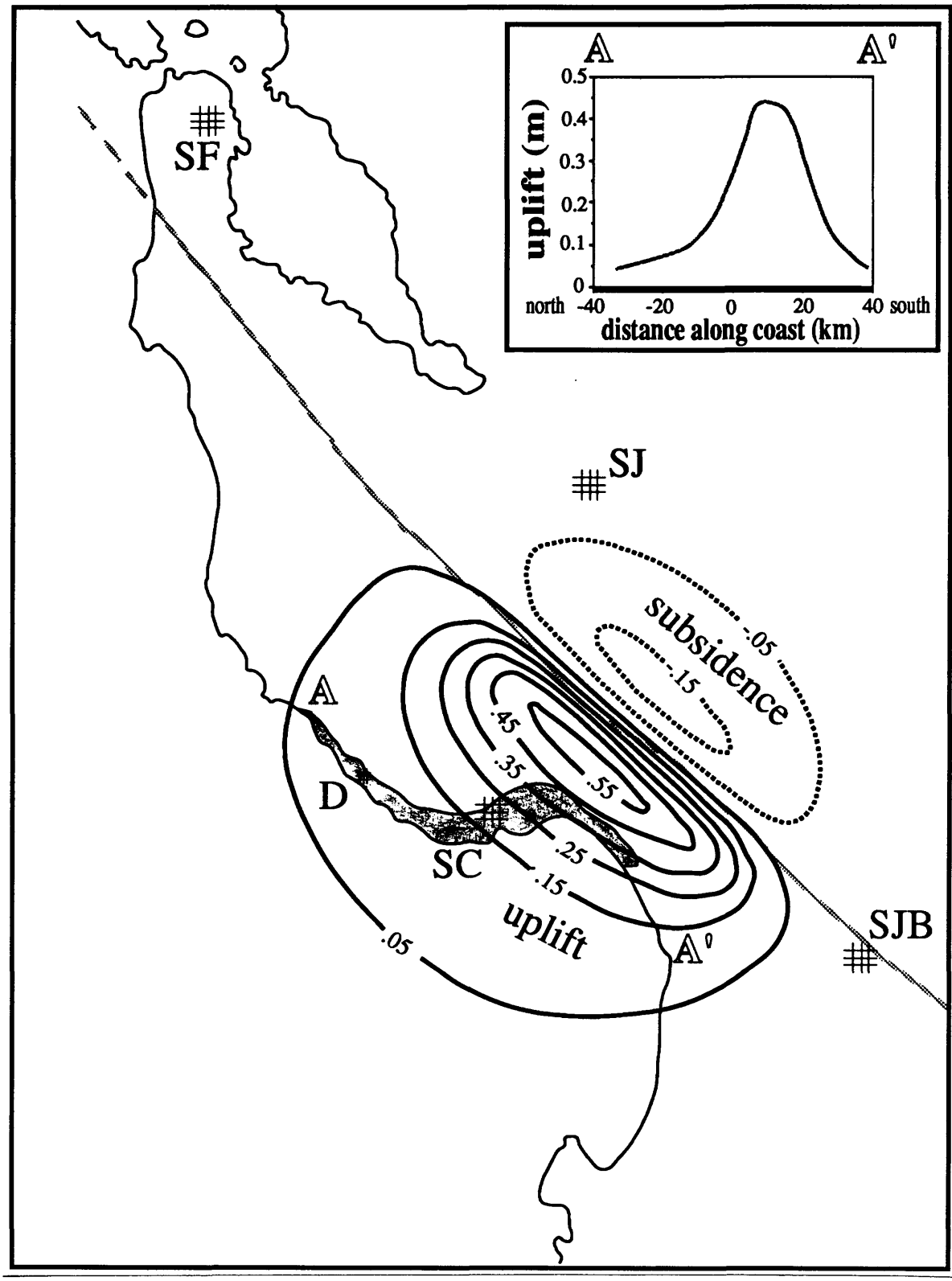

Figure 1.7 Distribution of uplift based upon laser geodometer and GPS measurements taken within days of the 1989 earthquake. Isolines of uplift in 10 cm intervals. Note slight subsidence expected on the North American plate east of the San Andreas fault, where the highest part of the Santa Cruz Mountain range exists. The shaded region along the coast depicts marine terrace deposits.

suggests that Loma Prieta itself subsided by roughly 13 cm with respect to landmarks well outside the uplift pattern during the Loma Prieta earthquake (Lisowski and others, 1990; McNally and others, 1989). This, too, suggests the existence of another type of seismic event; this one accomplishing uplift of Loma Prieta and the southern Santa Cruz Mountains further to the south. Detailed examination of the aftershock patterns associated with the Loma Prieta event has led to the suggestion (Schwartz and others, 1990) that the culprit is repeated events on the Sargent-Berrocal fault system.

Stop 2.
The Zayante-Vergeles fault zone

Kevin J. Coppersmith, Geomatrix Consultants

The Zayante fault zone is a major northwest-trending structural element of the Santa Cruz Mountains restraining bend. Beneath Quaternary alluvium of the Pajaro River, the Zayante fault presumably connects with the Vergeles fault in the northern Gabilan Range (Clark and Reitman, 1973). This fault zone is principally defined as the boundary between the Cretaceous crystalline rock of the Ben Lomond Mountain and Gabilan Range to the southwest, and a thick sequence of Tertiary rock to the northeast of the fault (Figure 2.1). Post-Paleocene vertical displacements are on the order of 2,000-3,000 m and locally up to 3,500 m.

The period of highest activity on the Zayante-Vergeles fault zone ended in Miocene time, but displacement has continued into late Quaternary and possibly Holocene time. Sedimentary rocks of the Purisima Formation, which are generally believed to be mid- to upper-Pliocene but are probably lower Pleistocene in this area, are vertically displaced about 200-400 m at various locations along the fault zone. Mid-Pleistocene Aromas deposits are displaced about 50 m

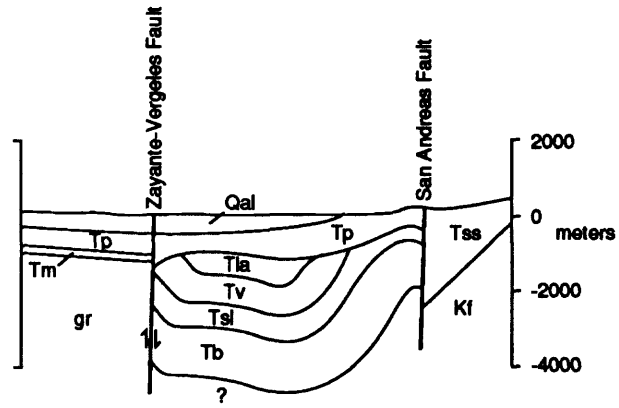

Figure 2.1 Generalized cross-section across San Andreas and Zayante-Vergeles fault. Qal - undifferentiated Quaternary deposits, Tp - Purisima Formation, Tm - Monterey Group, Tla - Lambert Shale, Tv - Vaqueros Sandstone, Tsl - San Lorenzo Formation, Tb - Butano Sandstone, Tss - undifferentiated Tertiary sediments, gr - Cretaceous granitic rocks, Kf - Franciscan Complex

and mapping of fluvial terraces (believed to be Sangamon or about 100,000 years old) in the Elkhorn River area indicates vertical displacement of about 5-15 m. True piercing points across the fault in Quaternary deposits have not been found to document the components of slip in the present tectonic environment. However, multiple measurements of slickensides and striae on fault surfaces in early Pleistocene to Holocene deposits suggest oblique reverse slip with the vertical and horizontal components of slip about equal. On the basis of displacements of mapped Quaternary surfaces, borehole data, and limited trench exposures (Figure 2.2), the estimated slip rate on the Zayante-Vergeles fault zone is about 0.2 mm/year.

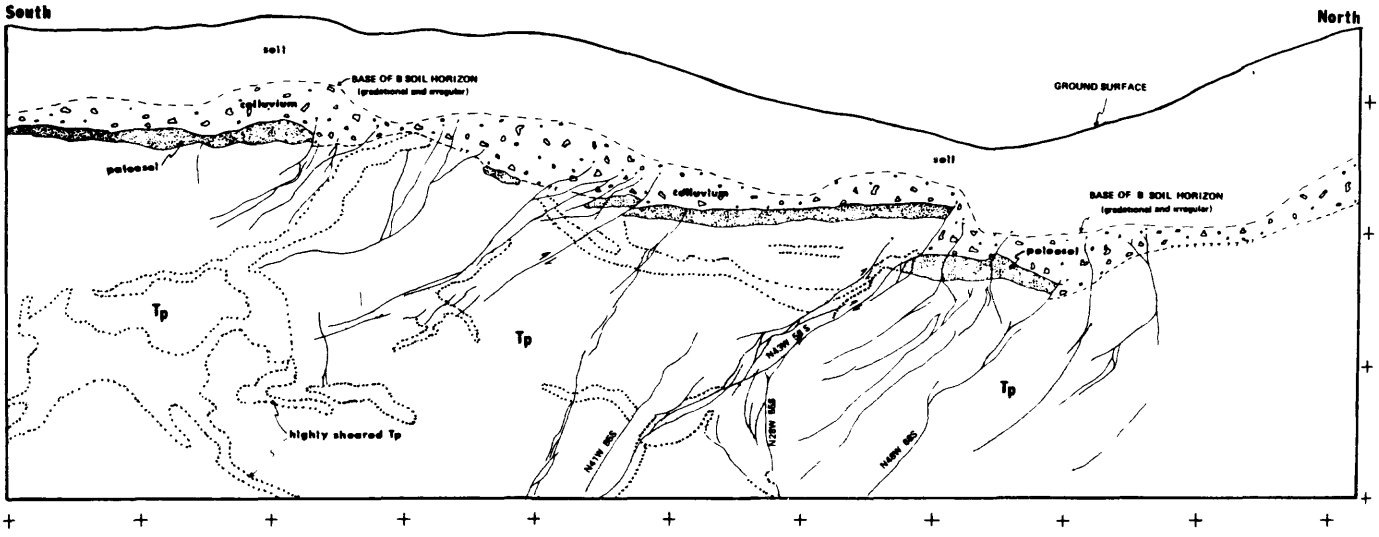

Figure 2.2 Log of Fern Flat Road exposure of Zayante-Vergeles fault zone. Tp represents Purisima Formation. Distance between crosses is one meter.

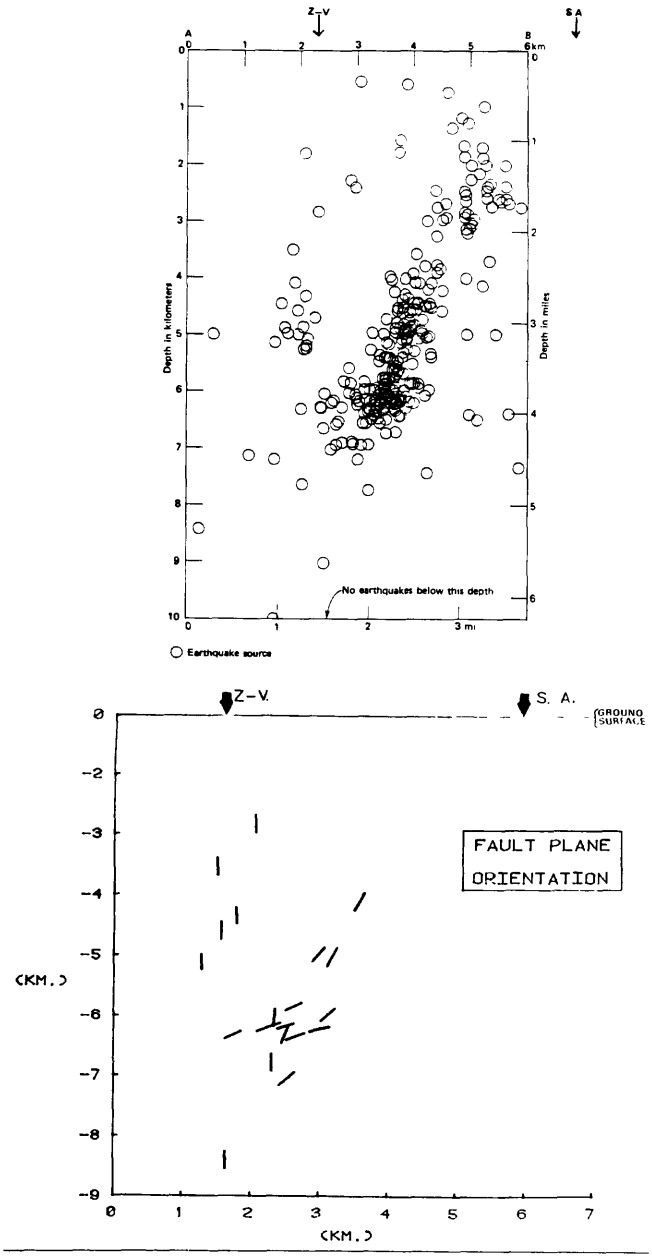

Figure 2.3 Upper figure shows hypocentral cross-section of events from 1969-1977. Lower figure shows fault plane orientation derived from fault plane solutions projected onto surface perpendicular to strike of Zayante-Vergeles and San Andreas faults. Arrows represent approximate locations of Zayante-Vergeles and San Andreas faults (from Coppersmith, 1979).

The Zayante-Vergeles fault is not obviously associated with historical or teleseismically recorded seismicity. Analysis of the post-1906 earthquake investigation given in the Lawson Report (Lawson and others, 1908) suggests that some of the field localities recorded by the field investigator, G.A. Waring, were along the Zayante-Vergeles fault. Whether or not the cracks and other deformation recorded at these sites represents sympathetic displacement on the Zayante-Vergeles fault during the 1906 earthquake is not known. A magnitude 5.2 aftershock of the Loma Prieta earthquake appears to have occurred in the Zayante fault area near Watsonville and 1989 ground cracks having right-oblique slip along Casserly Road, near Watsonville, seem to be unrelated to fill failures and other non-tectonic mechanisms. Therefore, sympathetic movement on the Zayante-Vergeles fault during the 1906 earthquake may have occurred. Instrumental seismicity in the region of the Zayante-Vergeles fault zone is diffuse. The systematic southwesterly offset of earthquake epicenters from the surface trace of the San Andreas fault in this area (Figure 2.3; Coppersmith, 1979) has always been attributed to problems in the velocity models used to locate earthquakes. However, the Loma Prieta event showed that southwest-dipping geometries of the San Andreas fault zone are real and are not simply related to velocity model problems. Hypocenter cross-sections of seismicity recorded between 1969 and 1977 (Coppersmith, 1979) clearly show a steep southwesterly dip on the San Andreas and a subvertical dip on the Zayante-Vergeles fault.

The geometry of the Zayante-Vergeles fault relative to the San Andreas fault zone and its sense of slip suggest that it is presently part of the accommodation of the restraining double bend in this part of the San Andreas fault system. The estimates of the Quaternary slip rate on the fault zone, as well as its poorly defined geomorphic expression, suggest that recurrence intervals for large earthquakes are probably one to two orders of magnitude longer than those for the San Andreas fault.

Olive Springs Quarry Exposure

We will stop at Olive Springs Quarry to observe structural and stratigraphic relations along the Zayante fault. The quarry operation is removing Cretaceous granitic rocks for road aggregate and other uses. These are exposed in the face of Sugarloaf Mountain on the southwest side of the fault zone. At the quarry, these granitic rocks are in contact with upper Pliocene to lower Pleistocene Purisima Formation rocks (Figure 2.4). Although the main fault is not presently exposed, shears can be observed in exposures of the intrusive rocks and sediments of the Purisima Formation. The Purisima Formation directly overlies the Aromas sands about 20 km south of this area and the Aromas is estimated to be about 700,000 to 1,000,000 years old. Therefore the Purisima Formation in this area may be early Pleistocene in age. Also exposed within the Olive Springs quarry is the fault juxtaposition of two distinctive units of the Purisima Formation: one a typical massive silty sandstone, the other an extremely clean silica sandstone.

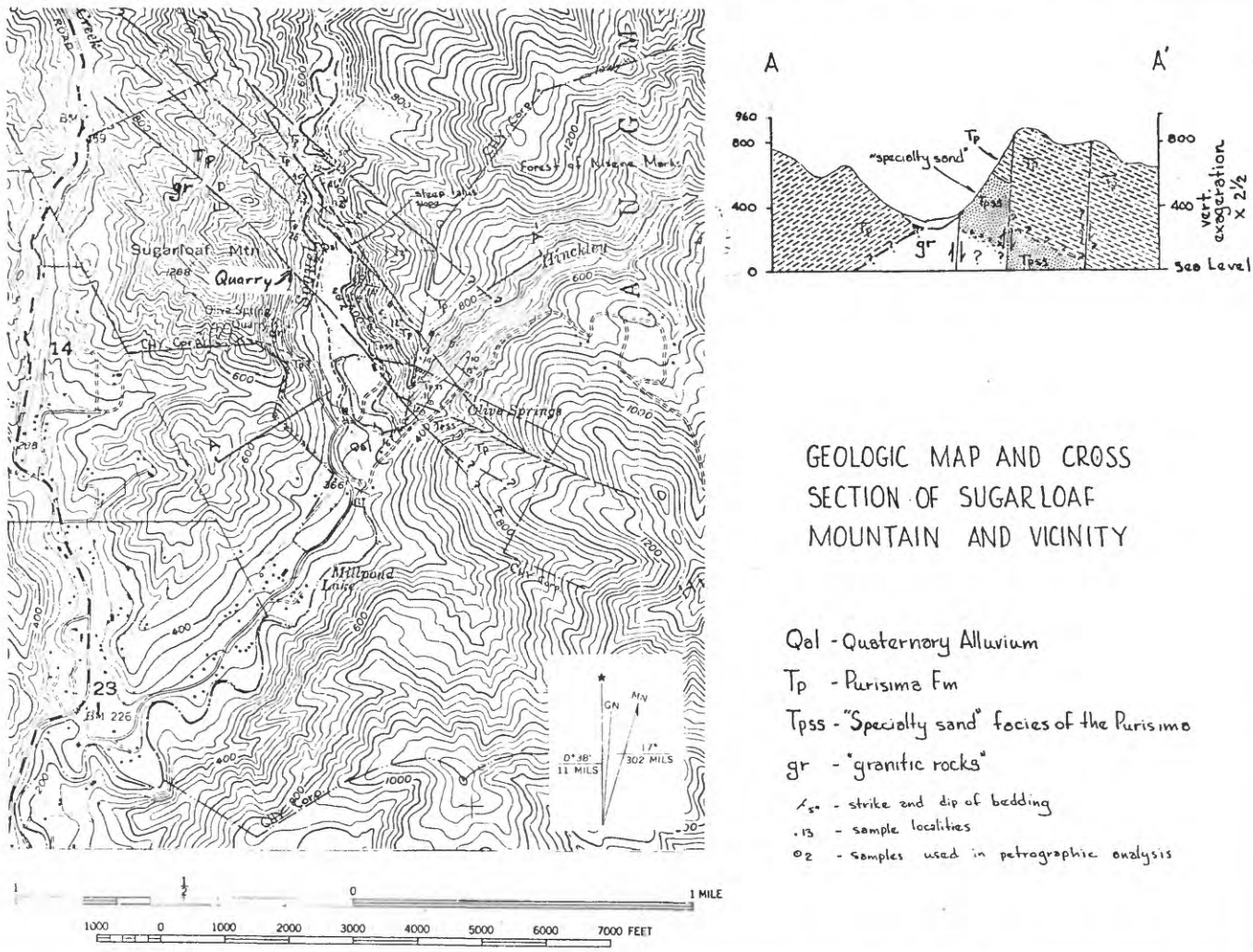

Figure 2.4 Geologic map and cross section of Sugarloaf Mountain and vicinity.

Stop 3.
The Morrell Cutoff Landslide: An Example of a Deep-seated Rotational Slump Triggered by the October 17, 1989, Loma Prieta Earthquake

E.L. Harp, USGS

One of the longest zones of earthquake-induced fractures makes up the headwall scarp of the Morrell Cutoff landslide (Figure 3.1). We have the opportunity to walk along the slide, observe the style of deformation, and compare this with cracks of possible tectonic origin at Stops 5 and 6. This landslide was first noticed crossing Morrell Cutoff Road about 0.6 km from its intersection with Summit Road. The scarp-forming cracks extended upslope from where they cross the Morrell Cutoff Road as a right-lateral shear. Here the zone of cracks passes through one of the gravel roads on a Christmas tree farm, forming an arc approximately 100 m in length. From the gravel road they extend almost 600 m to the east. Some of the largest cracks formed by the earthquake occur across the gravel road; here they are about 3 m deep and 1 m wide in places (Figure 3.2). Rather than a single fracture, the cracks define a zone containing several sets of fractures with downslope-facing scarps and extensive graben development between cracks.

South of where the lateral shear zone crosses Morrell Cutoff Road, the cracks make an abrupt change in azimuth from nearly N10°E to approximately N60°W and continue almost 200 m to the northwest before dying out. Along this northwest-trending section, the cracks exhibit upslope-facing scarps in places with up to 10 cm of vertical displacement.

Below the zone of cracks that form the headwall scarp of the landslide, the slopes range from 25° to 35°. About 60 m to the north of Morrell Cutoff Road below the arcuate zone of the scarps, slopes decrease in steepness and vary between 15° and 0°. Proceeding south across Morrell Cutoff Road toward the house on the Clindt property, we encounter the toe region of the landslide; the slope here is inclined approximately 5° to the north. South beyond the house, the slope steepens as we cross the toe of the landslide and observe a narrow zone of fractures that can be traced along the axis of the landslide toe for

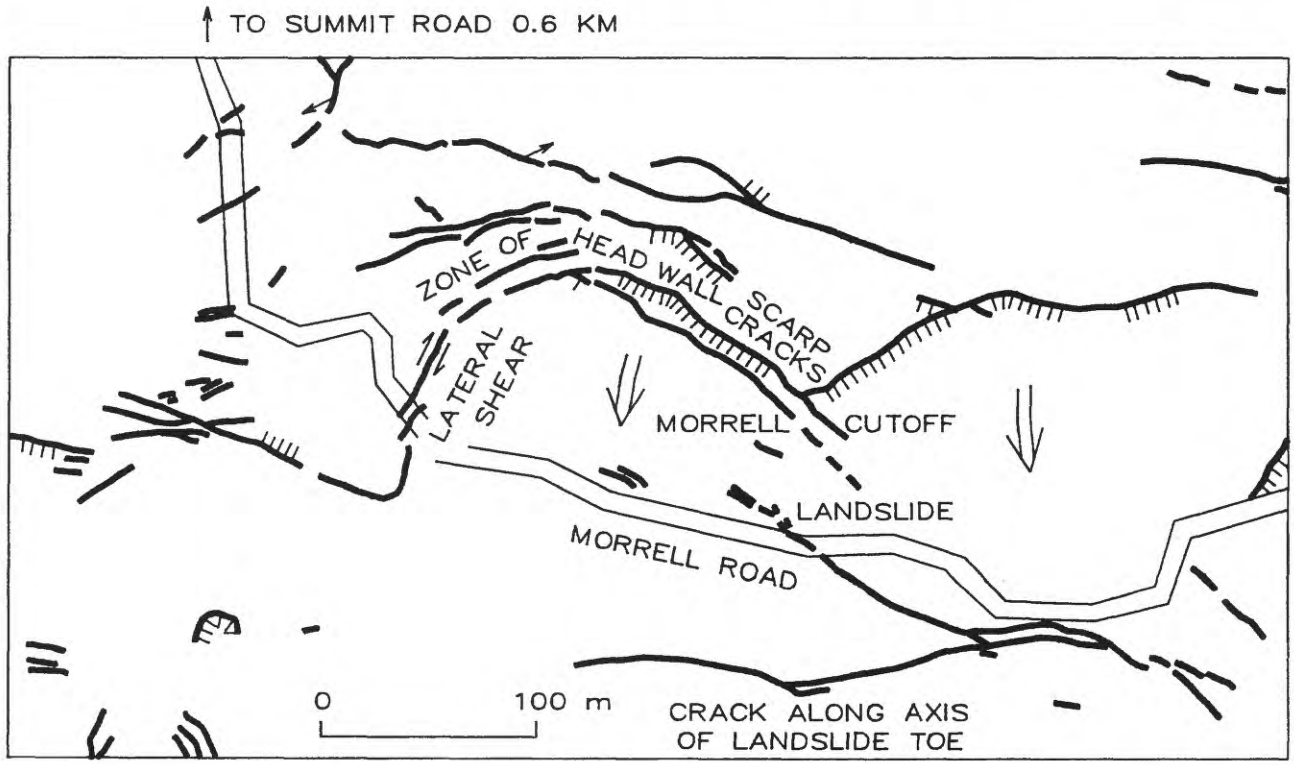

Figure 3.1 Map of fractures outlining the Morrell Cutoff Road landslide.

Figure 3.2 Cracks forming headwall scarp of Morrell Cutoff landslide.

Figure 3.3 Zone of fractures along axis of Morrell Cutoff landslide toe. View toward west.

Figure 3.4 Ridgecrest graben developed on landslide toe of Morrell Cutoff landslide. View to the east.

approximately 400 m; it then continues eastward across an open field, passing beneath several water tanks (Figure 3.3). East of the water tanks the cracks remain near the crest of the ridge created by the toe of the landslide. Here displacements were mainly extensional, 20 to 30 cm, and graben several meters wide developed between cracks (Figure 3.4). The cracks extend across a farm road and continue downslope toward Burrell Creek.

The origins of many of the numerous earthquake-induced ground cracks within the epicentral area near Summit Road are unclear. The patterns created by crack positions are, in many cases, confusing and do not suggest a single origin such as primary faulting, shaking-induced bedding slip, or landslide movement. The morphology of slopes involved in the fracture development and deformation of the Morrell Cutoff failure makes this example one of the few cases in which landsliding is an obvious origin. The Morrell Cutoff landslide is also one of the few in which the toe region was involved in noticeable deformation and displacement. On most other landslides in the Summit Road area, cracks that are believed to represent movement related to landslide processes are either associated with renewed movement at the headwall scarp or, less commonly, deformation along a lateral shear. Few locations have been observed within the epicentral area of the Loma Prieta earthquake where recognizable displacement has occurred in the toe region of a landslide.

The future stability of seismic-induced failures such as the Morrell Cutoff landslide is in question. Immediately after the earthquake, one of the greatest concerns was whether the triggered landslides would begin to move again if wet-season rainfall were to significantly raise water tables within the slide masses. Because of this concern, a geotechnical study of several of the large landslides and landslide complexes that affect residences and transportation routes has been funded by the Federal Emergency Management Agency (FEMA) to determine the present slope stability and to monitor subsurface pore-water pressures and subsequent movement. Due to the relatively dry winter of 1989-1990, the behavior of these large deep-seated landslides during high seasonal water tables has gone untested, and the long-term stability of many of the slopes in the Summit Road area remains unknown.

Stop 4.
Sargent fault zone at Loma Prieta

Robert McLaughlin, USGS

At this locality we will be standing on the top of Loma Prieta Peak, looking at the physiographically youthful trace of the Sargent fault where it crosses the divide between the headwaters of Los Gatos and Uvas Creeks. To the southeast the fault is geomorphically expressed as the deep, linear valley of Uvas Creek; to the northeast it is defined by a series of aligned notches separating late Cretaceous conglomerate from Eocene(?) marine sandstone and shale (Figure 4.1). It is unclear to what degree the geomorphic expression of the fault represents active tectonism or differential erosion. There are no studies that have demonstrated repeated late Quaternary displacements on the Sargent fault although the southern end near Pajaro Gap is marked by pre-1989 instrumentally recorded seismicity.

The Sargent fault zone at this locality appears to be composed of two main bedrock faults (Figure 4.1): 1) the youthful, steep, southwest-dipping fault that passes through the saddle in front of us and is geomorphically well-defined, and 2) an older, low-angle, southwest-dipping thrust fault that has displaced mafic basement rocks of the Jurassic Coast Range ophiolite northeastward over marine sandstone and shale of Early Eocene age. The low-angle fault passes to the north side of Loma Prieta Peak. These two faults probably merge at depth into an imbricate set of southwest-dipping reverse (thrust) faults (Figure 4.2). The Berrocal fault, located some 3 km northeast of the Sargent fault at Loma Prieta, and the Shannon fault, which occurs along the northeast range front of the Santa Cruz Mountains and displaces a paleosol that is younger than 20 ka, may also merge with this system of thrusts at depth. However, there is very little control on the downdip geometry and extent of the Sargent fault or the other reverse and thrust faults northeast of the San Andreas fault.

At Loma Prieta, and along strike to the northwest and southeast, the hanging wall and footwall rocks of the Sargent fault zone are hydrothermally altered. On Loma Prieta, this alteration includes the hydrothermal K-feldspar adularia, which we have dated by conventional K-Ar dating techniques at about 10 Ma. At another locality along the Sargent fault near Mount Madonna to the southeast, adularia is dated at 17 Ma. These ages indicate that hydrothermal circulation occurred along the Sargent fault between 17 and 10 Ma, and that the Sargent and related faults therefore had formed by 17 Ma (Middle Miocene time). Furthermore, contrasts in Miocene stratigraphy across the Sargent fault near Mount Madonna suggest that major uplift, erosion, and shortening occurred across the Sargent and Berrocal faults during Oligocene to early Miocene time. Plate tectonic reconstructions suggest that inception of the San Andreas fault system occurred at the restored latitude of these rocks at about 18 Ma. The Sargent fault and related southwest-dipping thrusts and reverse faults in this area therefore existed and probably formed at the time of initiation of the San Andreas fault system. This relationship deserves further careful study.

Activity during the 1989 earthquake

During the earthquake of October 17, no surface deformation occurred along this part of the Sargent fault. However, to the northwest, in the vicinity of Lake Elsman, near the intersection of the Sargent and San Andreas faults, considerable surface deformation was observed. Most of this consisted of extensional cracking, similar to the cracks in the Summit Road-Skyland Ridge area, although some noteworthy compression was noted along N40°-50°W-trending cracks. One prominent E-W-trending extensional crack within the Sargent

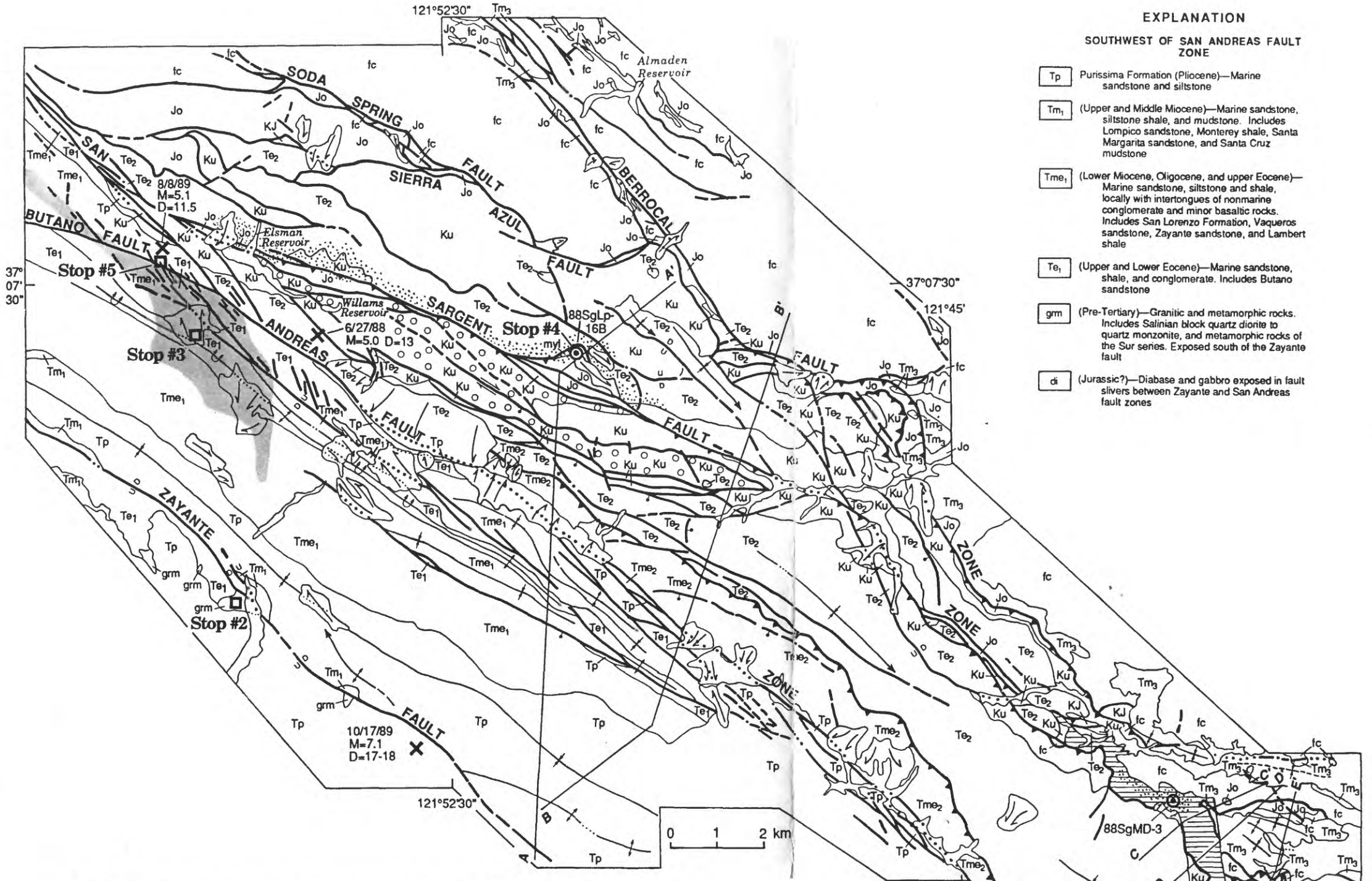

Figure 4.1 Geologic map of the Loma Prieta earthquake epicentral region, showing locations of mainshock of October 17, 1989 earthquake, the epicenters of the August 8, 1989 and June 22, 1988 earthquakes; the distribution of surface cracks which occurred on October 17, 1989, mapped by USGS Staff, 1989; geomorphically youthful fault features of the San Andreas system mapped by Sarna and others, 1975; and the principal bedrock trace of the San Andreas fault. Note that distribution of cracks does not closely correspond to the bedrock trace of the San Andreas fault, except locally. Geology simplified from maps of McLaughlin and others, 1988; Clark and others, 1989; Dibblee and Brabb, 1978; and unpublished mapping by McLaughlin, 1990. Locations of structure sections in Figure 4.2, and locations of K-Ar dates of hydrothermal alteration within Sargent fault zone are also shown.

EXPLANATION

SOUTHWEST OF SAN ANDREAS FAULT ZONE

- Tp — Purissima Formation (Pliocene)—Marine sandstone and siltstone
- Tm_1 — (Upper and Middle Miocene)—Marine sandstone, siltstone shale, and mudstone. Includes Lompico sandstone, Monterey shale, Santa Margarita sandstone, and Santa Cruz mudstone
- Tme_1 — (Lower Miocene, Oligocene, and upper Eocene)—Marine sandstone, siltstone and shale, locally with intertongues of nonmarine conglomerate and minor basaltic rocks. Includes San Lorenzo Formation, Vaqueros sandstone, Zayante sandstone, and Lambert shale
- Te_1 — (Upper and Lower Eocene)—Marine sandstone, shale, and conglomerate. Includes Butano sandstone
- grm — (Pre-Tertiary)—Granitic and metamorphic rocks. Includes Salinian block quartz diorite to quartz monzonite, and metamorphic rocks of the Sur series. Exposed south of the Zayante fault
- di — (Jurassic?)—Diabase and gabbro exposed in fault slivers between Zayante and San Andreas fault zones

NORTHEAST OF SAN ANDREAS FAULT AND SOUTHWEST OF SODA SPRING-SIERRA AZUL-BERROCAL-SARGENT FAULT ZONE

- Tme_2 — (Lower Miocene, Oligocene, and Upper to Lower Eocene)—Marine siliceous to carbonaceous shale and quartzofeldspathic sandstone. Exposed immediately northeast of San Andreas fault. Lower contact faulted
- Te_2 — (Middle? to Lower Eocene)—Marine quartzofeldspathic sandstone, siltstone, carbonaceous shale, and mottled mudstone. Base locally conglomeratic, glauconitic, and bioclastic
- Ku — (Upper Cretaceous-Campanian)—Marine arkosic wacke, shale, and pebble to boulder conglomerate
- KJ — (Lower Cretaceous to Upper Jurassic)—Marine shale, and minor sandstone, conglomerate, and tuff
- Jo — (Upper and Middle Jurassic)—Ultramafic and mafic to silicic igneous rocks of the Coast Range ophiolite. Also exposed locally northeast of the Berrocal fault zone
- myl — (Mesozoic?)—Mylonitic rocks associated with the Sargent thrust zone on Loma Prieta mountain

NORTHEAST OF THE SODA SPRING-SIERRA AZUL-BERROCAL-SARGENT FAULT ZONE

- Tm_3 — (Lower and Middle Miocene)—Marine sandstone and siliceous shale, locally conglomeratic and bioclastic at base. Siliceous volcanic rocks occur in lower part locally. Includes Temblor sandstone, Monterey shale, and younger, unnamed sandstone
- fc — (Pre-Tertiary)—Central belt of the Franciscan Complex-- Includes Upper Cretaceous Permanente limestone and basalt terrane, Upper Cretaceous to Middle Jurassic Marin headlands-Geysers chert terrane, and melange

SYMBOLS

- Contact—Dotted where concealed
- Anticline
- Syncline
- Fault—Dotted where concealed. Bar and ball on downthrown side, or (U) on upthrown side, and (D) on downthrown side
- Thrust fault or reverse fault—Sawteeth on hanging wall (upper plate) side
- 8/8/89 M=5.1 D=11.5 — Earthquake epicenter—Showing date of event, magnitude, and depth
- Landslide
- A A' — Line of structure section
- Main area of surface cracking associated with October 17, 1989 earthquake, from U.S. Geological Survey, 1989
- 88SgMD-3 — Area of hydrothermal alteration, showing locations of K-Ar ages from adularia
- Zone of complex fault imbrication (see cross section for geology)
- Stop #2 — Field trip stop

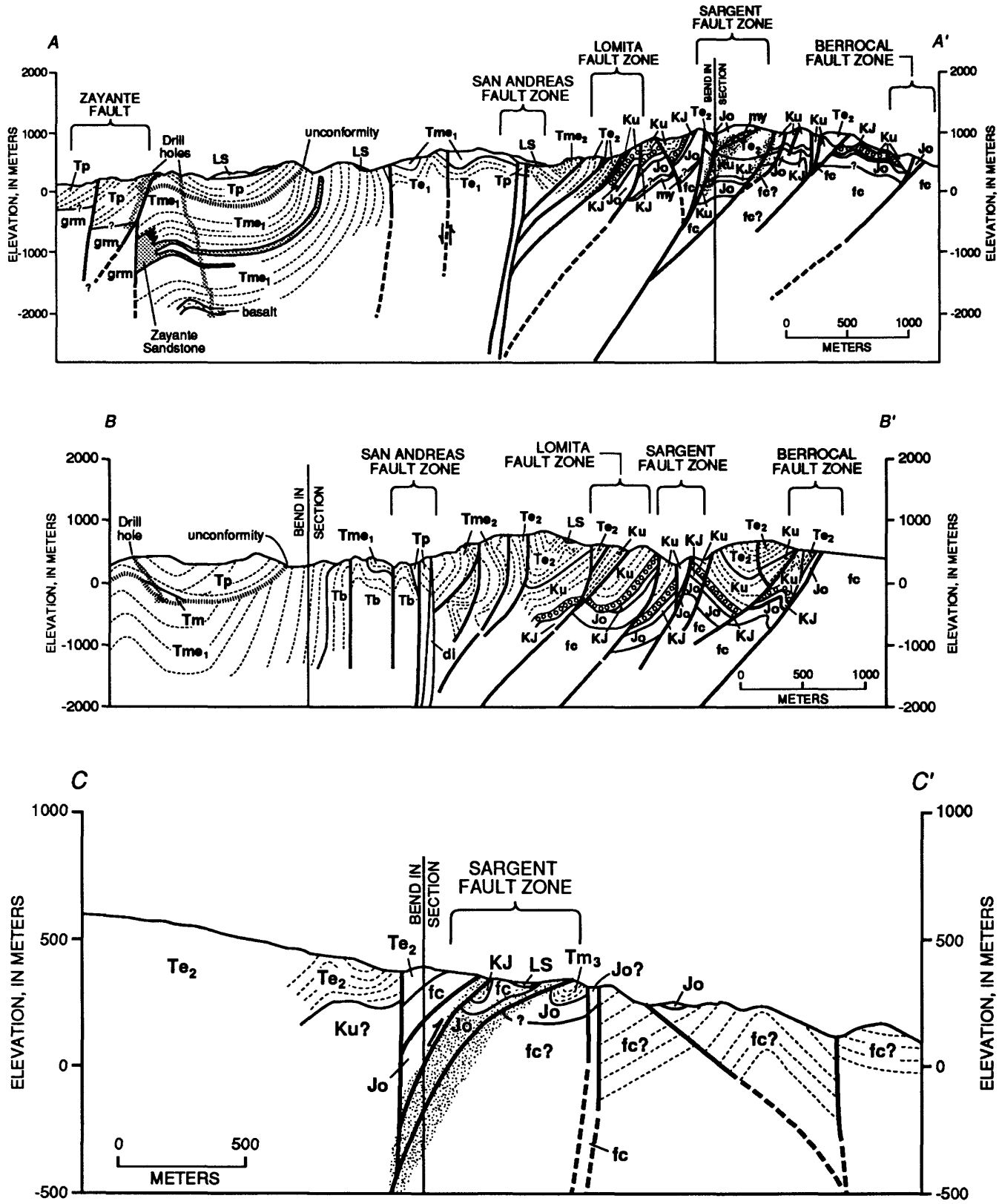

Figure 4.2 Structure sections across area of October 17, 1989 earthquake. See Figure 4.1 for explanation of map symbols. Note that scale of sections A and B differs from that of sections C, D, and E. Sections simplified and modified from McLaughlin and others (1988), and from McLaughlin (1971).

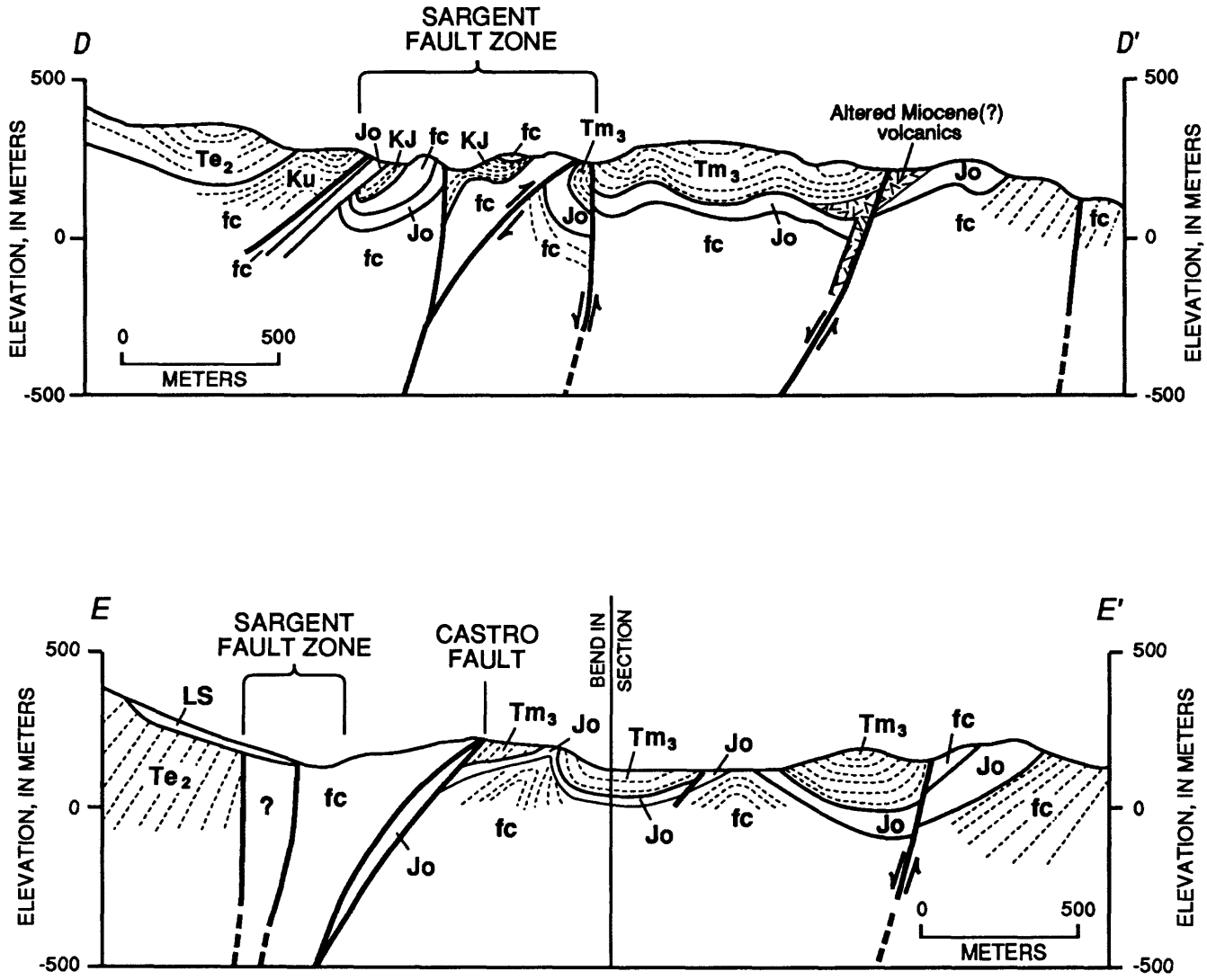

Figure 4.2, continued.

fault zone exhibited an oblique right-slip component of about 10 cm and an equal amount of vertical slip, with the southwest side down. Extensional separation on cracks in this area ranged from a few to as much as 31 cm.

The depth distribution of aftershocks following the October 17 earthquake (Figure 4.3) shows a distinct alignment of hypocenters defining the steeply southwest-dipping fault plane that ruptured. The aftershocks propagated to within a few kilometers of the surface, just south of the surface trace of the Sargent fault. These data suggest that the earthquake occurred on a southwest-dipping, blind, dextral-reverse-slip fault that attempted, but failed to propagate to the surface along the Sargent fault. It is likely that that the Sargent fault and other minor structures between it and the San Andreas fault, such as the Lomita fault, were sources of much of the shallow aftershock activity.

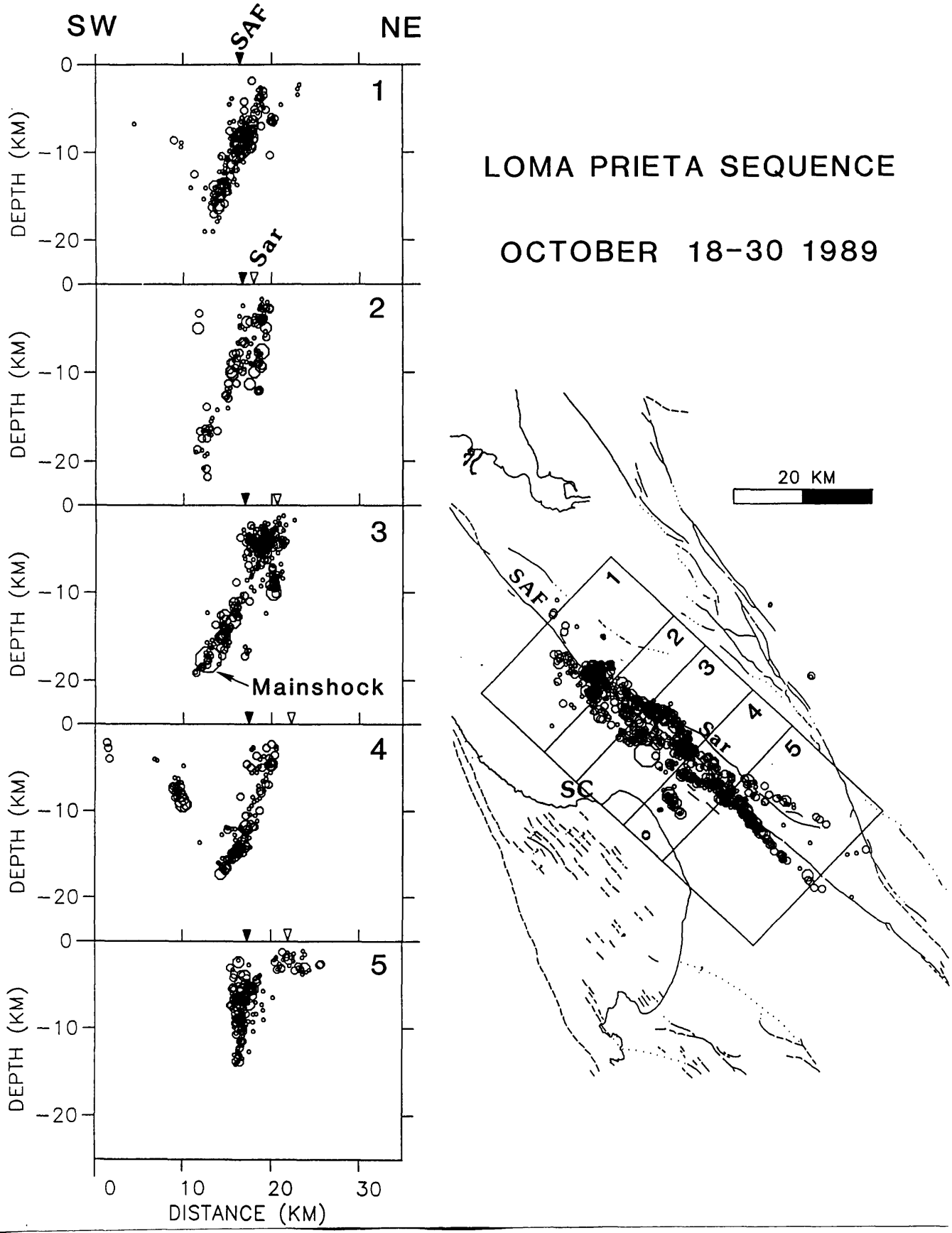

Figure 4.3 Map and cross-sections of seismicity (October 18-30, 1989) associated with the Loma Prieta earthquake. Numbered boxes on map outline regions that are plotted individually on cross sections (from Dietz and Ellsworth, *in press*).

Stop 5.
Morrill Road
Surface fractures associated with the 1906 and 1989 earthquakes

Daniel J. Ponti, Carol S. Prentice, David P. Schwartz and Ray E. Wells, USGS

Part A. 1906 and 1989 surface fractures compared

Carol S. Prentice and David P. Schwartz, USGS

Here at Morrill Road two fractures with left-lateral and vertical displacements were well documented in the Lawson Report of the 1906 earthquake (Lawson and others,1908), and both fractures moved in a similar fashion in 1989. These have now been patched but the cracks can still be traced off road, particularly in the orchard (soon to be a Christmas tree farm) to the southeast. This is the only locality where surface cracks documented in the Loma Prieta area in 1906 can be directly compared with measurements made in 1989 (Figure 5.1). In 1906, the larger of the two cracks (the northeastern fracture) showed left-lateral displacement of 1.1 m. The 1989 displacement was not as large; measurements made the morning after the earthquake, before road repairs, showed 41 cm of left-lateral displacement, 33 cm of extension, and 10 cm of vertical displacement (Figure 5.1; Table 2). Although this is the only locality specifically documented in the Loma Prieta area in 1906, extensive fracturing in the Summit Road and Skyland Ridge areas was also described. Fracturing similar to that described in 1906 was observed after the Loma Prieta earthquake in the same areas. Another potential locality for comparing displacements is the Wright's tunnel: deformation of the tunnel was documented after the 1906 earthquake, but the tunnel is now closed; the possibility of reopening it to determine if any deformation occurred in 1989 is being studied.

Careful review of the Lawson Report (Lawson and others, 1908) raises an important question about the Loma Prieta segment of the San Andreas fault: was there tectonic surface rupture on the main trace of the San Andreas fault in this area in 1906? Fault displacement associated with the 1906 San Francisco earthquake in Marin County and the San Francisco peninsula was generally very well documented in the Lawson Report. However, the investigation in the southern Santa Cruz Mountains is an exception. The investigator, Stanford student G.A. Waring, apparently veered away from the main trace of

A

Figure 5.1 Larger of two cracks that broke Morrill Road by left-lateral motion in both 1906 San Francisco earthquake and 1989 Loma Prieta earthquake. *A*, View southwest across Morrill Road in 1906 showing left-lateral displacement of 3.6 feet (Lawson, 1908, plate 65A). *B*, Same crack on October 18, 1989, morning after earthquake, before road repairs, showing 1.1 feet of extension, 1.2 feet of left lateral displacement, and 0.3 feet of vertical displacement. Yardstick is aligned in direction of movement of opposite sides of crack. *C*, View of present-day Morrill Road (October 1989) similar to 1906 view after asphalt road had been patched, showing left-lateral displacement of edge of road.

B

C

Figure 5.1, continued.

the San Andreas fault and may have missed a long section of the main trace between Summit Road ridge and Pajaro Gap (Figure 5.2). The locations of most of the fractures described in the report are poorly documented. The report mentions only four sites of horizontal offset southeast of Lyndon Canyon: the Wright's tunnel, the Morrell ranch, the Pajaro River railroad bridge, and a fence halfway between Chittenden and San Juan. The Lawson Report clearly indicates about 1.5 m of right-lateral offset within the Wright's tunnel, but not on the surface above it. The Morrell Ranch fractures are the left-lateral fractures described above, and clearly do not represent surface rupture on the San Andreas fault. The report describes damage to the Pajaro River railroad bridge, but does not clearly document actual fault displacement. Deformation of the railroad bridge, which was also reported following the 1890 earthquake that occurred between Pajaro Gap and San Juan Bautista, may be shaking induced. The report describes 1.2 m of horizontal offset of a fence halfway between Chittenden and San Juan, but does not give a specific location or sense of offset, nor does it characterize its relationship to the fault trace.

In summary, we simply do not know with certainty what happened in 1906. There are no observations in the 1906 report that unequivocally demonstrate that surface faulting occurred in the Santa Cruz Mountains and extended as far south as San Juan Bautista. In light of the 1989 observations it is possible to infer that there was no surface faulting in this region in 1906; therefore, the 1906 observations might best be explained as secondary tectonic and shaking features. Alternatively, there is enough uncertainty, including the observational gap, such that the occurrence of surface faulting south to San Juan Bautista in 1906 cannot be excluded. Perhaps the surface rupture was intermittent and small to begin with and was obscured by landslides and other ground failure features.

The Loma Prieta earthquake—a characteristic event?

Was the Loma Prieta earthquake a characteristic event? This question has been asked repeatedly since the earthquake. It is also a question for which there is no immediate answer. A characteristic earthquake implies that the amount of slip during repeated large earthquakes on a fault segment is essentially the same (Schwartz and Coppersmith, 1984). For Loma Prieta much depends on how one interprets the amount of slip during the 1865 and 1906 events. Intensity data from the 1865 earthquake (Toppozada and others, 1981) suggest that it ruptured approximately the same segment of the fault zone as the 1989 event and, by inference, was essentially the same size. As discussed, the fault may or may not have ruptured the surface in 1906, and the amount of slip that occurred at depth is highly uncertain. Using geodetic data, Thatcher and Lisowski (1987)

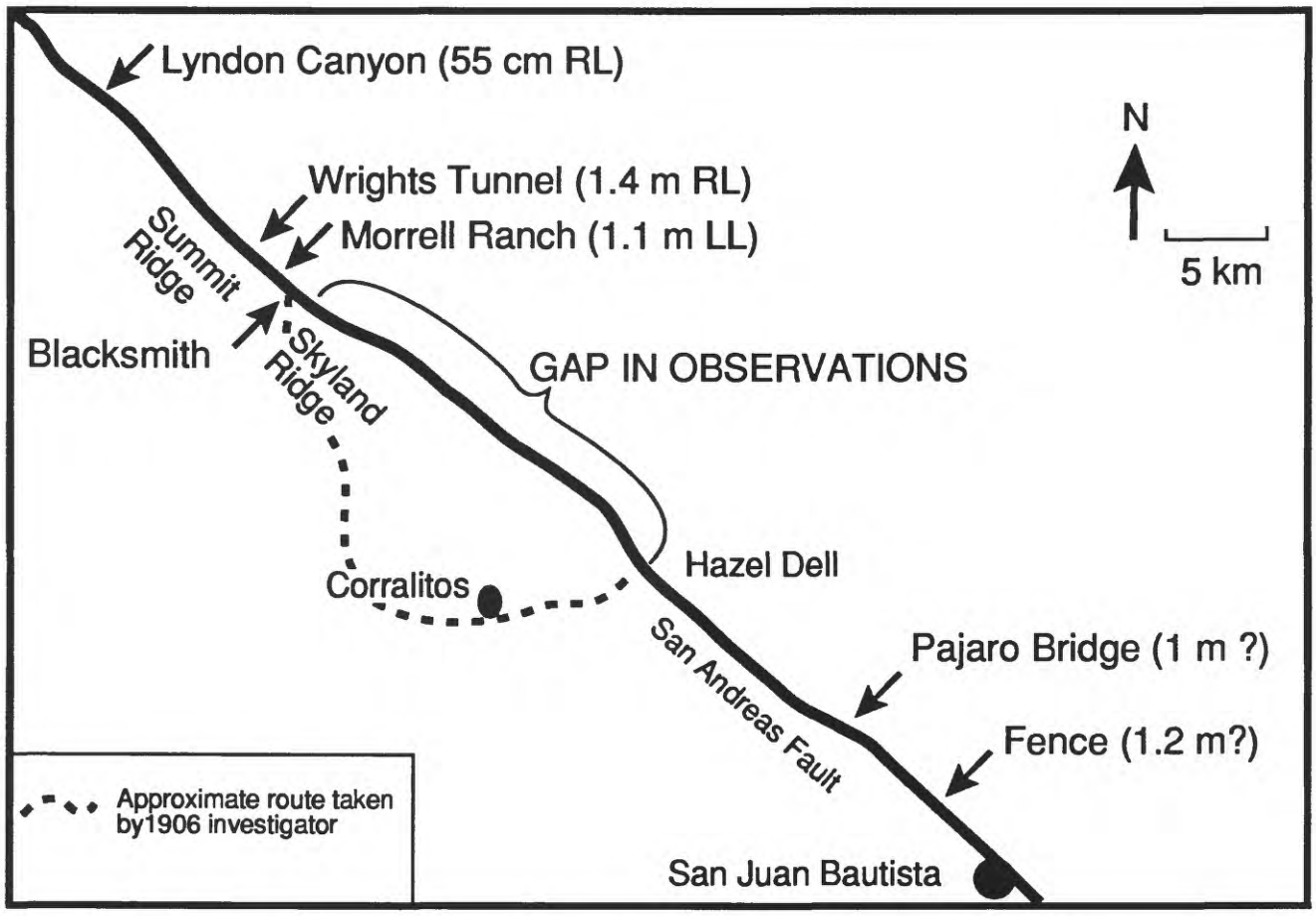

Figure 5.2 Map showing locations between Lyndon Creek and San Juan Bautista mentioned in 1906 report and visited by 1906 field investigators.

estimated 2.6 m of right-lateral slip at depth in 1906, whereas the Wright tunnel offset suggests 1.5 m of near-surface offset. If there was no surface faulting in 1906 and 1989 (and possibly 1865), and if the amount of slip was similar, one might conclude that this part of the fault fails with a characteristic deep slip that has lateral and vertical components similar in value to the 1989 offset.

A variable rupture mode and downdip segmentation are required to explain the behavior of this segment of the fault if the upper 5 km of crust slipped in 1906 or if the fault has ruptured to the surface during the recent geologic past. Certainly the youthful geomorphic expression of the linear San Andreas rift valley, with right-laterally deflected drainages and sag ponds, indicates recent and recurrent surface faulting. In this case it is probable that the fault fails in at least two ways (Figure 5.3). The first failure mode would be deep (18 km) nucleation within the segment (such as in 1989 and possibly 1865) with upward termination of the rupture at a depth of 5-6 km. The upward termination may be controlled by a structural or geometric barrier at the intersection of the San Andreas and Sargent faults (Figure 5.3). In a second rupture mode, the fault fails in response to a large rupture that nucleates outside the segment (such as in 1906) and propagates laterally into it at shallow (< 10 km) depths. In this case the San Andreas-Sargent fault barrier could be bypassed and the shallow section of the fault would rupture to the surface, possibly releasing some stress stored from 1989-type events. Whether a laterally propagating rupture would also result in slip on the deeper fault surface is conjectural. Its downdip extent may depend on the actual slip distribution of the 1989-type event (Figure 5.3), which is unknown at present. In fact, a shallow event (~10 km) nucleating within the southern Santa Cruz Mountains segment is another possibility.

In the case of a variable rupture mode, the events nucleating within the segment may be true characteristic earthquakes. It is unclear whether the amount of shallow slip associated with

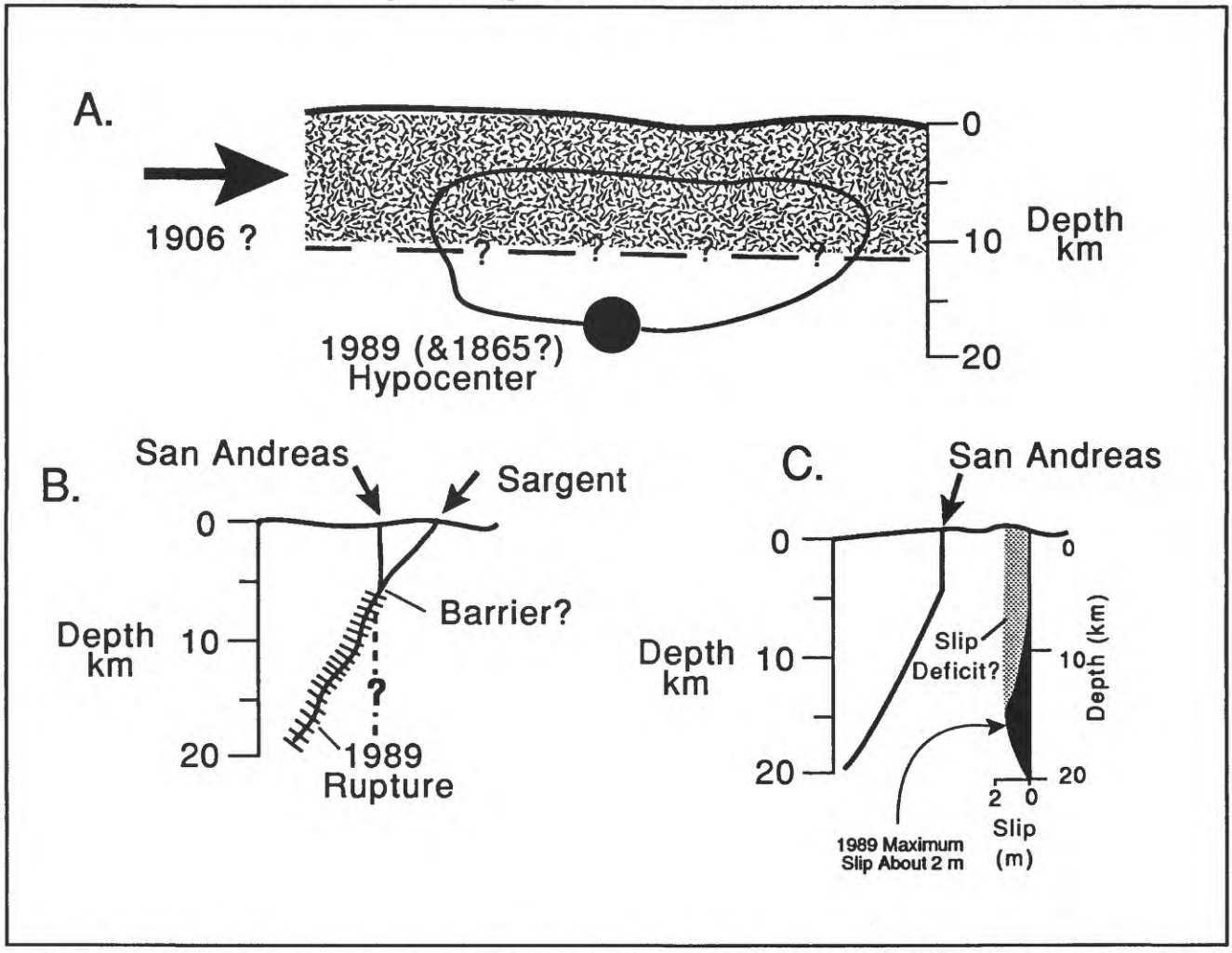

Figure 5.3 Schematic diagrams showing possible characteristics and controls of slip in the Santa Cruz Mountains. *A*, Santa Cruz Mountains segment fails in two ways: 1) a deep rupture that nucleates within the segment and 2) a shallow rupture that nucleates outside of the segment and propagates in laterally. Queries indicate uncertainty in downdip extent of shallow rupture. *B*, Possible control of upward termination of 1989 rupture by barrier defined by intersection of San Andreas and Sargent faults. Queried line is downdip projection of a vertical San Andreas fault. *C*, Slip distribution from 1989 (hypothetical) could control downdip extent and behavior of ruptures associated with the shallow San Andreas fault. Stippled band is possible slip deficit zone that will be filled in by the next earthquake.

a rupture propagating laterally into the segment represents only a release of the stress accumulated to that point in time or if it is partially a function of the size of the "push" it receives. These are intriguing concepts that have been raised as a result of the Loma Prieta earthquake. Clearly, a variable mode of the rupture has important implications for the way in which slip parameters, particularly offset values from this earthquake and 1906, are used to forecast the future behavior of this and adjacent segments of the San Andreas fault.

Part B. Extent and origin of surface fractures in the Summit Road–Skyland Ridge area

Daniel J. Ponti and Ray E. Wells, USGS

The Morrill Road fractures are significant because, as described above, the very same cracks displayed similar, although larger, displacements during the great San Francisco earthquake of April 18, 1906 (Lawson and others, 1908). Of all of the 1989 surface ruptures, only at Morrill Road can we positively demonstrate prior coseismic movement. But are the Morrill fractures and other similar fractures in the Summit Road and Skyland Ridge areas a result of tectonic deformation, or are they simply due to gravitational failure invoked by strong ground motion? The origin of the Summit Road–Skyland Ridge fractures is complex, and no single explanation can account for all of the observed ground cracks. In the following paragraphs we will discuss the character of these features and discuss some of the possiblities for their formation.

General character of the Morrill Road and other surface fractures

The general location of the Morrill Road fractures, their overall orientation, and their senses of displacement are typical of most of the other coseismic fractures in the Summit Road and Skyland Ridge area. The main fracture crosses Morrill Road approximately 120 m north of the intersection with Summit Road and extends continuously in a southeastward direction for nearly 600 m (Figure 5.4); evidence of this frac-

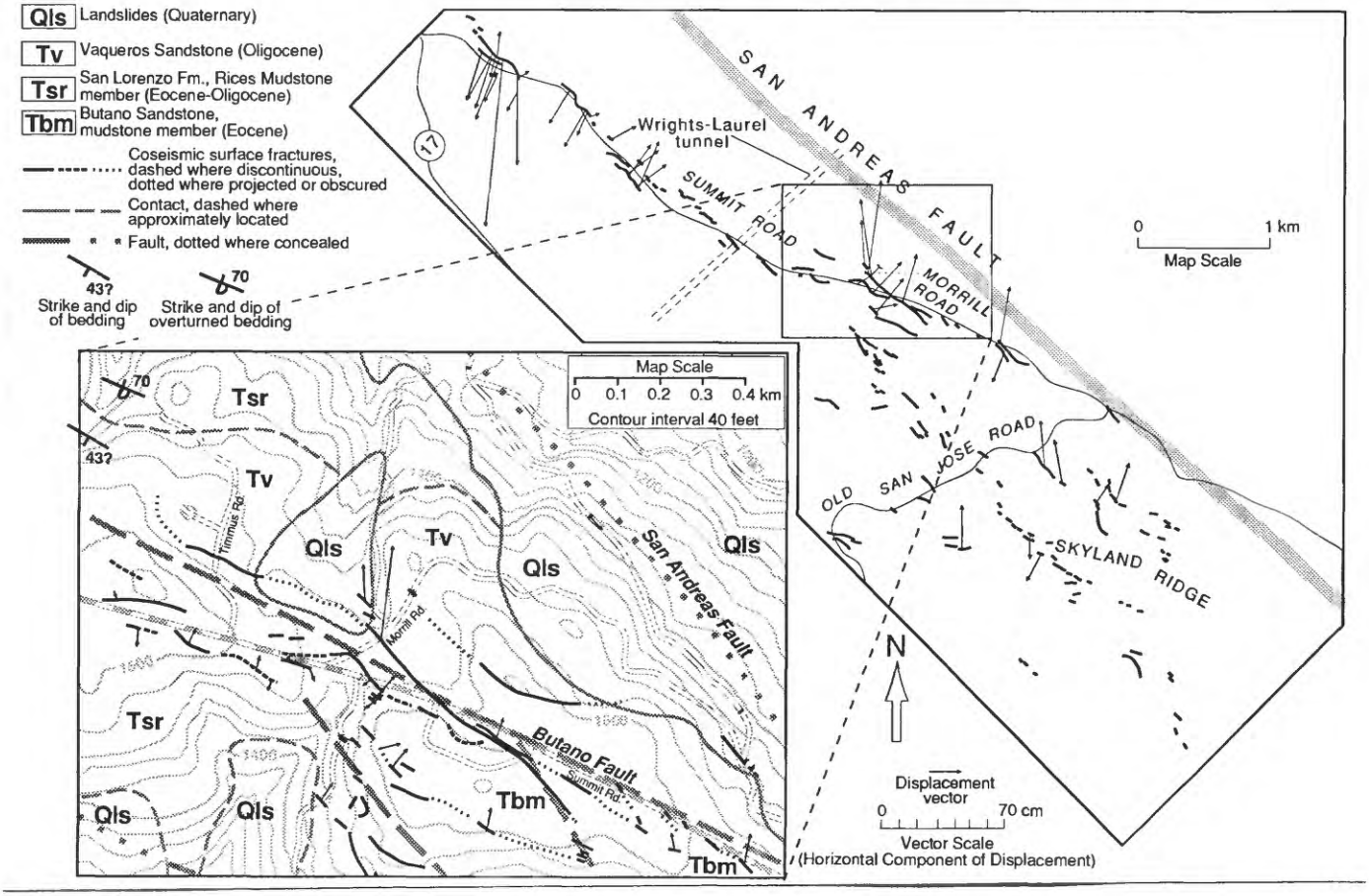

Figure 5.4. Map showing zones of prominent surface fractures and selected net displacement vectors produced in the Summit Road - Skyland Ridge area of the Santa Cruz Mountains during the Loma Prieta earthquake; inset shows geology, surface fractures, and measured displacement vectors in the vicinity of Morrill Road. Open cracks obviously related to local slumping or large landslides are not shown. The location of the surface trace of the San Andreas fault is determined by the 1906 offset in the Wrights-Laurel tunnel and by topography and bedrock mapping. Lengths of the displacement vectors correspond to the horizontal component of measured displacements as indicated by the vector scale; arrows point in the plunge direction. Mapped fractures from USGS Staff (1989); geology from Dibblee and Brabb (1978) and Clark and others (1989); topography and culture from USGS Los Gatos (1980) and Laurel (1968) 7.5' quadrangle maps.

TABLE 2.

	Main Fracture	Secondary Fracture
Maximum Measured Total Displacement (mm)	540	169
Max. Extensional Component (mm)	334	108
Max. Lateral Component (mm)	412	6
Max. Vertical Component (mm)	103	129
Fracture Azimuth	N 32° W	N 50° W
Displacement Vector Azimuth (Plunge Direction)	N 7° E	N43° E
Displacement Vector Plunge	11°	50°
Sense of Lateral Motion	Left-Lateral	Right-Lateral

ture is still apparent in the orchard east of Morrill Road. Northwest of Morrill Road, the displacements are smaller and the cracking becomes discontinuous. It is difficult to ascertain the westernmost limit of the fracture, although it appears to trend into the headwall scarp of a possible landslide near Timmus Road, located 600 m to the northwest. This fracture is the longest continuous rupture mapped in the area and exhibits the second largest displacement (54 cm) of any fracture system in the region; most fractures show displacements of 10 cm or less. The smaller of the Morrill Road fractures crosses the road approximately 30 m north of the intersection of Morrill and Summit roads and has an overall length of about 200 m. This fracture trends more westerly than the main fracture, although it does bend sharply to the southeast as it crosses Summit Road. Detailed displacement data for the two Morrill fractures are given in Table 2.

The Morrill Road fracture system occurs near the center of an 8 km by 2 km area that is located near the northern end of the subsurface rupture zone, along the southwest side of the projected surface trace of the San Andreas fault (Figure 5.4). Nearly all of the major Santa Cruz Mountains fractures are confined to this relatively small region. As is typical of most Santa Cruz Mountains fractures, the Morrill Road cracks trend NW-SE, and displacements are primarily extensional in a NNE-SSW direction. Most fractures in the region display significant components of lateral slip, commonly left-lateral slip, and the Morrill Road fractures are no exception.

As can be observed in the adjacent orchard, the Morrill fractures follow a distinctive break in slope and occur along the margin of a shallow linear depression; this feature is apparently associated with the Butano fault as mapped by Dibblee and Brabb (1978). Many other cracks in the Summit Road area also follow similar topographic features although most do not occur in association with any recognized bedrock faults. The association of many of the cracks with these types of landforms indicate that the local topography formed by repeated movements along these fracture zones. Based on the fact that the Morrill Road fractures moved coseismically in 1906, it is likely that prior movements on this and other fracture systems were also earthquake-induced.

The location and orientation of most fracture systems appear to be controlled by bedrock lithology and geometry, and their displacement azimuths are closely associated with local or regional slope directions (Figure 5.5). While some fractures, such as those at Morrill Road, are associated with known geologic structures, most are not. Most fractures occur within steeply dipping, relatively incompetent rocks, such as the mudstone units of the San Lorenzo Formation and the Butano Sandstone, and shale interbeds of the Vaqueros Sandstone (Clark and others, 1989; Dibblee and Brabb, 1978; USGS Staff, 1990b; Cotton and others, 1990). In the general case, fractures are aligned with the regional strike of bedding; where specific fractures were measured, fully 75% lie within 35° of the local strike of bedding. In rocks that are highly anisotropic with respect to their materials properties, such as the Vaqueros Sandstone, it is clear that fractures are largely confined to bedding planes (Figure 5.6).

Possible mechanisms for the formation of the Summit Road–Skyland Ridge fractures

The Summit Road surface fractures probably formed as a result of: 1) strong ground motion that resulted in large-scale slumping of the hillsides and/or collapse of the ridge crests, and 2) tectonic uplift and extension of the hanging-wall block due to fault movement at depth. There is little evidence to suggest that the lateral components of motion observed on many of these fractures are due to tectonic shearing. The displacements of most fractures can be associated with local or regional slope failures, or dip-slip faulting along bedding planes. Several lines of evidence support both ground motion and tectonic mechanisms for the formation of the fractures in the general case, and it is likely that both mechanisms played a role in producing the features we see. Data that suggest a tectonic origin are not as well supported, however, except in the case of some specific fracture systems. Various arguments that support both views are summarized in the following paragraphs.

The surface fractures are confined to a region that was apparently subject to the most severe ground motions. The greatest damage to competent structures, the largest number of topped trees, and the highest density of displaced boulders and landslides occurred within the very same localized region where the most prominent surface fractures formed; this relationship could therefore support the theory that fracturing was initiated by severe ground shaking. However, the location of the fractures can also be used to argue for a tectonic origin; nearly all of the major fractures occur southwest of the San Andreas fault and are therefore located on the block that was apparently subjected to uplift during the earthquake. The absence of fracturing on the northeast side of the San Andreas

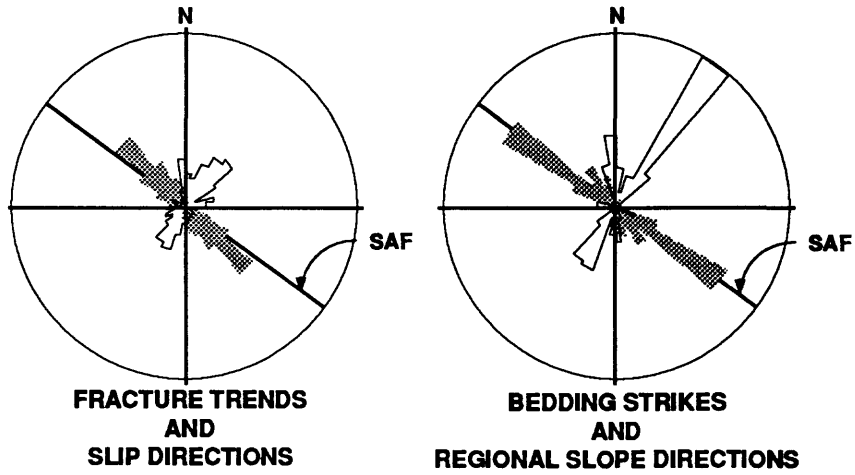

Figure 5.5. Rose diagrams of fracture trends, displacement vector azimuths (slip directions), bedding strikes, and regional slope directions in the Summit Road - Skyland Ridge area. Radius of each circle represents a frequency of 24%; Diagonal line on both plots depict the azimuth of the slip plane of the Loma Prieta earthquake (Plafker and Galloway, 1989). Diagram on left depicts trends of fractures (grey) and slip vector azimuths (black outline) obtained from 200 measurement stations located on the fractures. Diagram on right depicts strikes of bedding (grey) obtained from 47 localities (data from Dibblee and Brabb, 1978; Clark and others, 1989; Brabb, unpublished), and regional slope directions, as derived from ridge-crest azimuths (black outline), that correspond to the 200 measurement stations. Note the similarities between the fracture azimuths and strike of bedding, and between the slip vector directions and regional slope directions. These data suggest that fracture trends are controlled by bedding and that movement on the fractures generally parallel regional slope. Movement on many of the Summit Road fractures, therefore, appears to be due to gravitational failure of the ridge tops, probably due to shaking. The dominant NNE-SSW trend to the regional slope as compared to the NW-SE trend of bedding also explains the tendency for many fractures to exhibit left-lateral motion.

fault, however, may simply be caused by the fact that the sandstones and Franciscan complex rocks there are more competent than the Tertiary sediments found southwest of the fault, and are therefore less likely to fail during shaking events.

A shaking origin is also supported by the observation that most fractures occur at or near the tops of ridges, particularly fractures with large displacements such as those along Summit Road. Nearly 3/4 of all the measured displacements indicate movement downslope; for the majority of those fractures that show downslope movement, the trends of the displacements (the displacement vector azimuths) correlate strongly with either the local or regional slope (Figure 5.5). Displacement on the Morrill Road fracture system, for example, appears to be best related to downslope movement.

Not all fracture systems follow ridge crests, however, and not all displacements can be explained by downslope movement. Several prominent fracture systems cross Laurel Canyon west of Old San Jose Road and cut obliquely across Skyland Ridge. Several crack systems in this and other areas appear to be associated with mapped bedrock faults or fold axes (Clark and others, 1989; Dibblee and Brabb, 1978; Sarna-Wojcicki and others, 1975). One such series of small extensional fractures occurs along the mapped trace of the axis of the Laurel anticline. The Laurel anticline fractures have displacements that are generally small (median displacement is 46 mm), have little or no vertical component of motion (median plunge angle is 5°), and nearly half of the measured displacements have no apparent slope control. Of all of the fracture systems within the Summit Road-Skyland Ridge area, these are the best candidates for a tectonic origin; they could be bending-moment faults (Yeats, 1986) which formed as a result of extension over the crest of the anticline as it was further compressed.

Extension across a fold axis or tectonic displacement of bedrock faults are not the only ways to explain the existence of fractures that are located near such features, or that have displacements that are not slope-controlled. For example, the Morrill fractures are closely associated with the mapped trace of the Butano fault (Dibblee and Brabb, 1978; Figure 5.4), yet given that the sense of displacement on the Morrill fractures is closely related to the local slope, it appears unlikely that the Butano fault moved tectonically during the October 17 earthquake. Rather, the fault probably acted as a zone of weakness whereupon gravitationally-induced failure occurred. Most of the observed fractures with uphill-facing scarps cannot be bending-moment or flexural-slip faults because they exhibit displacements that are not compatible with those models. Many of these fractures probably resulted from strong ground shaking which caused failure along weak bedding planes due to lateral movement of ridge flanks and collapse of the ridge crests.

Another argument that can be used to support the theory that strong ground motion accounts for many of the displacements lies in the amount of cumulative extension exhibited in the fractures along Summit Road and on Skyland Ridge. Individual fractures in the Summit Road area are observed to have as much as 60 cm of extension (USGS Staff, 1989), and numerous others display several tens of centimeters of extension; estimates of total extension across the region, therefore, are upwards of several meters. Given that current geodetic models predict a maximum uplift of only around 35-45 cm in the Summit Road region, it is unlikely that tectonic extension due to uplift across a broad arch would alone result in such large displacements.

Finally, many large fracture systems appear to be intimately related to large slide complexes. Several fracture systems trend into headwall scarps of pre-existing landslide masses. These slide complexes are common along both flanks of the Summit Road and Skyland ridges and many of them were reactivated by shaking during the October 17 event.

The surface ruptures in the Summit Road-Skyland Ridge area represent an aspect of earthquake hazards that has not, up until now, been fully appreciated. Regardless of their origin, the hazard posed by these fractures to structures, roads, and pipelines is significant. While it is apparent that there is a significant gravitational component to many of these fractures, we do not know whether tectonic uplift across the region is required for their formation. If uplift is a requirement, then we may be looking at a hazard that is unique to this region of the San Andreas fault and may not be an important factor in other areas. If, however, these fractures are primarily shaking-induced, as appears likely, then we might expect similar fractures to form in response to earthquakes along other reaches of the San Andreas, such as on the Peninsula segment, or along other faults where geologic and topographic conditions are similar to those in this portion of the Santa Cruz Mountains.

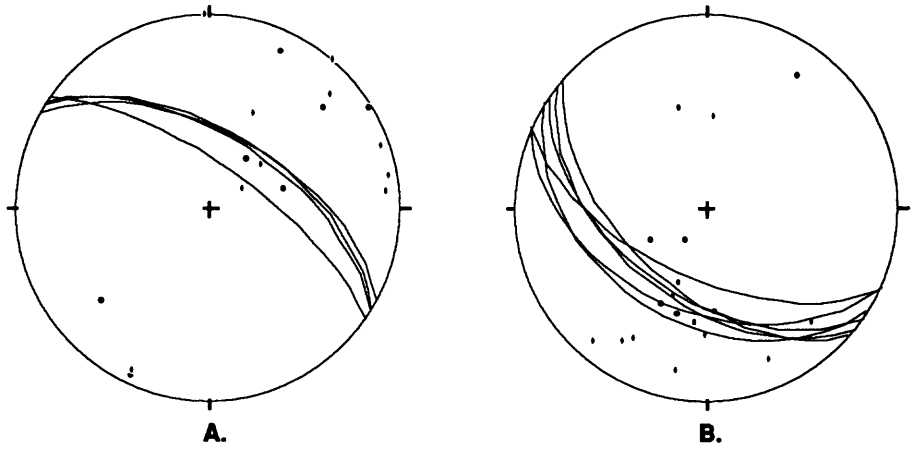

Figure 5.6. Equal area stereographic projections of bedding within the Vaqueros Sandstone (great circles) and displacement vectors (dots) for several large fracture systems that formed adjacent to Summit Road 0.5 to 2 km southeast of Highway 17; many of these fractures have uphill-facing scarps. Stereonet A shows bedding and displacement vectors for the fracture systems located on the southwest limb of a syncline. Bedding here strikes NW and dips to the northeast; nearly all displacement vectors also plunge northeast. Stereonet B shows bedding and displacement vectors for fracture systems located on the northeast limb of the same syncline. Here bedding dips to the SW and most of the displacement vectors plunge to the SW as well; many lie on or near the bedding planes. These data suggest that failure on these fracture systems occurred within the bedding planes during lateral spreading of the the ridge flanks and collapse of the ridge crest.

Stop 6.
Highway 17 Deformation

William R. Cotton, William Cotton and Associates

The Highway 17 site is located on top of a cutslope approximately 1.5 km to the southwest of the mapped trace of the San Andreas fault and approximately 300 m to the northeast of the Butano fault. Here we have the opportunity to observe structural and lithologic features that may control the sense of displacement and location of at least some of the ground cracks that formed in the Summit Road–Skyland Ridge area. The day following the earthquake, two cracks were observed across the pavement of Highway 17. Both could be traced into the shale interbeds within the Vaqueros Sandstone. The dark unit on the opposite cutslope is the wider of the two shale interbeds (Figure 6.1). The cracks extended a short distance to the east, and continued to the west (behind us) for about 100 m. In addition to the cracks, the northbound and southbound lanes of the highway as well as the concrete median divider and the guard rail behind us were buckled across the entire width (about 10 m) of the shale interbed. Net vertical displacement across the zone was 40 cm down to the north.

The primary zone of recent faulting is defined by a 15-cm-wide zone of clay gouge that parallels bedding (N55°W, 60°N) and has been mapped through the exposures on both sides of the road. Near the top of the eastern (opposite) cutslope, the fault displaces an 8-m-thick, charcoal-rich deposit of surficial materials that appears as a tan wedge within the top of the shale interbed (Figure 6.2). The lowermost 2 m of the deposit is displaced by several subsidiary faults, indicating that the primary fault plane has experienced multiple episodes of normal slip. Our preliminary geologic logging of the fault relationships indicates that buried paleosols and colluvial wedges may exist within the surficial deposit that will provide further evidence for multiple faulting events. Carbon samples for radiometric dating have been obtained. Because the observed 1989 displacement on this fault was clearly coseismic, we believe that investigation of these features will provide important data on the timing and magnitude of paleoseismic events on the Santa Cruz Mountain segment of the San Andreas fault.

The surficial materials cut by the fault are interpreted to have formed as infill deposits of a fault-bounded, ridge-top depression. Similar topographic depressions are present along the ridgecrest to the east and have been previously mapped (Sarna-Wojcicki and others, 1975). The origin of the depressions and associated topographic furrows and scarps that

Figure 6.1 Southeast view of the bedding plane-normal fault relations in the Highway 17 roadcut. Faulting bisects a thick shale unit (dark band) in the Vaqueros Sandstone (light areas) and can be traced to within one meter of the ground surface. An 8-meter thick cover of surficial materials, believed to be infill of a ridge-top depression, is displaced by the fault.

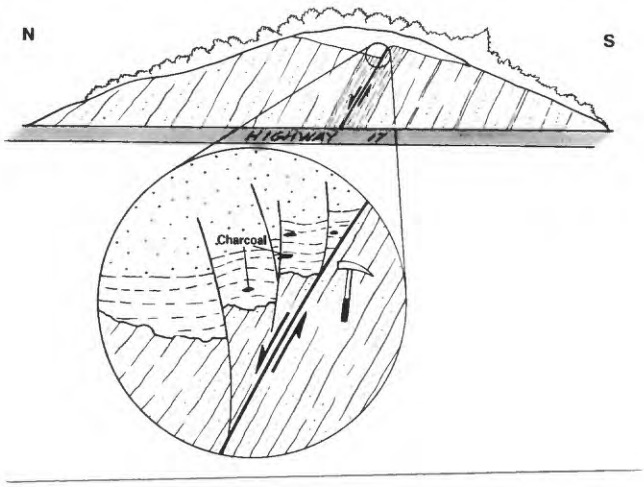

Figure 6.2 Diagrammatic cutslope geology along Highway 17 at Summit Road and details of fault relationship between bedding plane fault and young surficial deposits (inset).

characterize the Summit Ridge area is believed to be the result of repeated second-order faulting.

Based on the observations at Highway 17 and at other locations in the Summit Road area, we believe that the best working hypothesis to explain the origin, orientation, and distribution of both pre-existing ridge-top depressions and the many ground fissures that developed along the crest of the Summit Ridge area as a result of the 1989 Loma Prieta earthquake is bedding plane faulting characterized by predominantly normal slip. The orientation and distribution of the bedding plane faults are, in turn, controlled by the lithology and structure of the bedrock and, specifically, the location of the weak shale interbeds. It is our working model that faults like the bedding plane fault identified at Highway 17 are analogous to second-order, bending-moment faults related to coseismic, active folding processes as described by Yeats (1986).

Bending-moment faults result from lengthening (i.e., tensional-normal faults) of the convex side of a folded layer and corresponding shortening (i.e., compressional-thrust faults) of the concave side of the fold. An example of this model is the 1980 Algerian earthquake on the El Asnam fault where displacement on the main seismogenic thrust was accompanied by active anticlinal folding, which was, in turn, accompanied by graben development along the anticlinal crest (Yeats, 1986).

In the Summit Ridge area, it is our hypothesis that the ridgecrest was lengthened and normal faulting occurred along pre-existing planes of weakness in the bedrock such as bedding planes, faults and fractures. The extension of the ridgecrest was due to tectonic arching of this portion of the Santa Cruz Mountains that occurred in association with the earthquake.

In our model, the 1.3 m reverse-slip and 1.9 m right lateral oblique strike-slip that occurred at depth did not extend into the upper 6 km of the crust (Lisowski and others, in press), but was accommodated at the ground surface by extensional faulting along bedding planes and other weak bedrock structures on the southwest side of the fault zone (i.e., hanging-wall block), and possibly by compressional tectonics (i.e., foot-wall block). The vertical deformation of 1.3 m at depth translated into approximately 36 cm of uplift at the ground surface (Plafker and Galloway, 1989). The uplift was not concentrated along the trace of the San Andreas fault as primary ground rupture, and therefore, must have been partially accommodated by slip along weak discontinuities within the bedrock.

With regard to compressional tectonics, evidence for shortening as a result of the Loma Prieta earthquake has been documented in the Los Gatos area situated north of the fault (see Stop 7). It is also well-expressed in the geologic record by the Sargent-Berrocal, Shannon and Monte Vista faults that define the zone of range-front faulting along the north side of the Santa Cruz Mountains (McLaughlin, 1974; McLaughlin and others, 1988; Dibblee and Brabb, 1978; Sarna-Wojcicki and others, 1975). The Santa Cruz Mountains have attained their present elevation by thrusting Franciscan bedrock to the north over Quaternary alluvial deposits of the Santa Clara Valley.

We propose that a model incorporating bending-moment faults characterized by extensional tectonics in the hanging wall block and compressional tectonics in the footwall block can account for: 1) the ground fissures in the Summit Road ridge area, 2) the geomorphology of the Summit Road ridge area, 3) the compressional ground deformation documented along the Santa Cruz Mountains rangefront, 4) the system of rangefront faults along this segment of the fault, and 5) the lack of primary right-lateral ground rupture along the trace of the San Andreas fault.

Stop 7.
Coseismic ground deformation along the northeast margin of the Santa Cruz Mountains

R. A. Haugerud and S. D. Ellen, USGS

Northeast of the San Andreas fault are several sub-parallel, generally southwest-dipping faults (Figure 7.1). Among these are the Monte Vista fault (Dibblee, 1966; Sorg and McLaughlin, 1975), Berrocal fault and Shannon fault (Bailey and Everhart, 1964), and the Sargent-Berrocal fault zone (McLaughlin, 1974; Sorg and McLaughlin, 1975). The presence of older rocks in the southwest sides (hanging walls) of most of these faults suggests some component of reverse-slip or thrust motion, a sense of motion consistent with uplift of the Santa Cruz Mountains relative to the Santa Clara Valley.

Published maps show some of these faults to involve semi-consolidated gravels of the Santa Clara Formation and thus to have been active in the last million years (Cummings, 1968). William Cotton and Robert McLaughlin (oral communications, 1989) report that a recent foundation excavation in Los Gatos exposed a fault placing Franciscan Complex rocks above young alluvial deposits, suggesting younger Quaternary

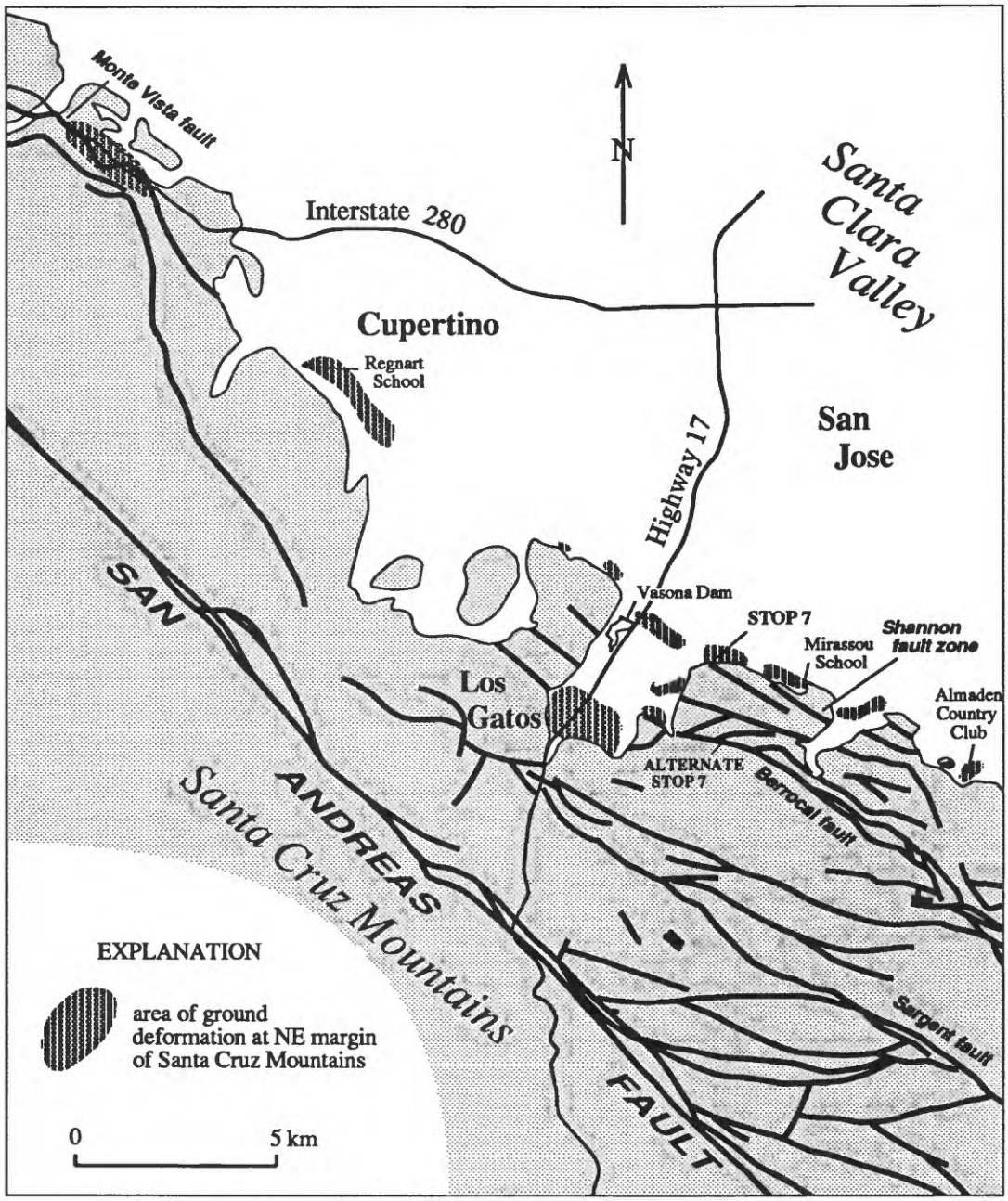

Figure 7.1. Map showing extent of observed ground deformation on northeast margin of Santa Cruz Mountains following the Loma Prieta earthquake. Bedrock and older alluvium shaded; selected faults shown only where they cross bedrock or older alluvium.

activity. Another recent excavation along the Shannon fault near New Almaden showed that a paleosol estimated to be ~20 ka is cut by a segment of the Shannon fault (R. McLaughlin, J. Hardin, oral communications, 1990).

Deformation during the Loma Prieta earthquake

After October 17, freshly-broken and buckled concrete curbs, gutters, and sidewalks were abundant in places along the northeast margin of the Santa Cruz Mountains. A concentration of breaks on N-S streets near the foot of Blossom Hill defined a linear zone (the Blossom Hill zone) that was largely continuous from Mirassou School in easternmost Los Gatos to near Vasona Dam on Los Gatos Creek, a distance of about 4 1/2 km (Figure 7.2). Within this zone, most visible deformation was compressional and limited to a belt less than 300 m wide. Most gaps in the zone correspond to areas without concrete sidewalks, curbs, or gutters. We found similar deformation to extend intermittently to the southeast as far as the Almaden Country Club and northwest to Regnart School in Cupertino, for an overall length of ~20 km. Scattered pavement deformation along and near Interstate 280 as far north as

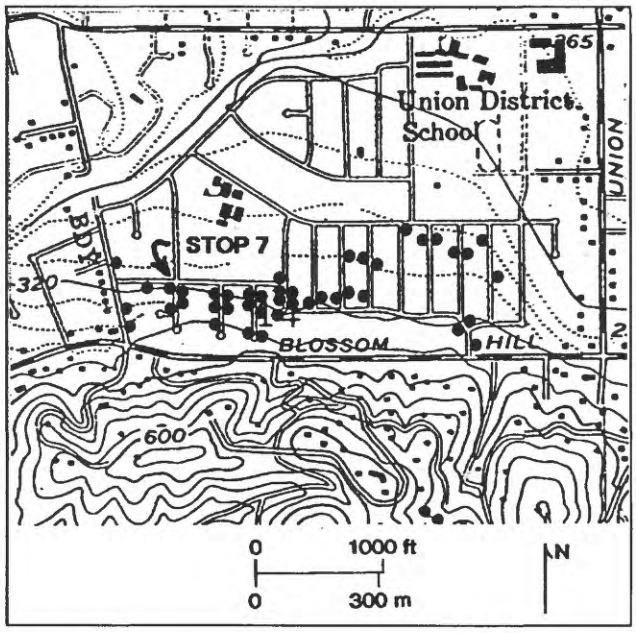

Figure 7.2. Map of area around stop 7, north of Blossom Hill Road and west of Union. Black circles mark freshly deformed pavement following the Loma Prieta earthquake.

Page Mill Road in Palo Alto may be a continuation of this zone, though north of Cupertino failure patterns were more complex and suggestive of strike-slip faulting.

A second major zone of compressional deformation passed through downtown Los Gatos (Figure 7.1). It was about 1 km wide and nearly continuous along strike for the 2 1/2 km where concrete strain markers are present. Concrete curbs and sidewalks broke and buckled throughout much of downtown Los Gatos. Many boxes for underground utility connections and meters were shortened northeast-southwest so that their lids no longer fit. Northeast-southwest shortening was also evident from failures of the concrete median and asphalt paving on Highway 17. Continuous concrete slabs along Los Gatos Creek where it flows through town provided an unusually good strain marker. Overlaps at three discrete breaks in the slabs along the southeast bank of the creek showed a total of 20-25 cm of northeast-southwest shortening.

Most of the evidence for deformation in these zones was freshly broken or buckled concrete, typically curbs or sidewalks (Figure 7.3). Adjacent asphalt typically showed little obvious deformation. In most places strains appear to have been very small, near the elastic limit of concrete: fractured curbs on one side of a street in many places lacked corresponding fractures on the other side. Failures were typically compressional, commonly suggested net shortening, and most were on north- to northeast-trending curbs and sidewalks. Eyewitness reports and our observations indicated that such deformation in both zones was largely coseismic, but that locally in the Los Gatos zone similar deformation both predated and postdated the earthquake by as much as several weeks or months. Lawson and others (1908, p. 274) described "about a dozen upheavals of sidewalks, mostly on north and south streets" in Los Gatos during the 1906 earthquake.

Cause of deformation

Broken and buckled pavement in the Los Gatos zone was associated with permanent shortening. The distribution of deformation and direction of failure are inconsistent with the effects of differential compaction or local slope failure. Deformation must have been tectonic, but we cannot yet associate it with a discrete fault—our concrete strain markers may also be good stress guides, so that the breaks may not coincide with the locus of deformation in the underlying earth. However, deformation was spread over a large enough cross-strike distance that surface deformation probably does not reflect slip on a single fault surface at shallow depths. Perhaps deformation reflects genuine pervasive shortening, as in the core of a synform or relaxation of a preexisting bulge; alternately, it might reflect slip distributed on several discrete surfaces.

The cause of deformation in the Blossom Hill zone is less certain. Temporary, elastic, deformation during the earthquake is one possibility. Slope failure is not plausible in the flat terrain between Blossom Hill and Los Gatos Creek. Differential compaction of unconsolidated deposits (the thickness of which probably changes across the Blossom Hill zone) should produce dominant extension. Tectonic shortening seems the most likely cause; however, many compressional failures have associated local extension, and measurements have not yet unequivocally demonstrated net shortening.

In places the zones of coseismic deformation coincide with mapped strands of the Sargent-Berrocal, Shannon, and Monte Vista faults. Elsewhere they do not, which might indicate that the deformation is not fault-related, but more likely reflects our imperfect knowledge of the poorly-exposed geology of the Santa Cruz Mountains foothills.

An example from the Blossom Hill zone

This stop is reached by taking Highway 9 (East Los Gatos) exit from Highway 17 and proceeding east on Highway 9 about 0.4 mile to Los Gatos Boulevard. Turn left (north) onto Los Gatos Boulevard, go about 0.8 mile to fourth stop light, and turn right (east) onto Blossom Hill Road. Follow Blossom Hill Road 1.1 miles to Camino del Cerro; turn left (north) onto Camino del Cerro; go 2 blocks on Camino del Cerro to Westchester and turn right (east) onto Westchester. Go 2 blocks and turn right (south) onto Dover Street. Follow Dover Street south 1 block to its intersection with Blossom Glen Way and park. At this point we are at the foot of Blossom Hill, the northeastern-most ridge of the Santa Cruz Mountains at this latitude.

Note the broken concrete curb at the SW corner of the intersection. The curb is similarly broken one block south, at the NW corner of the intersection with Dover Court, and compressional failure is evident in the curb along the west side of Dover Street, but no deformation is evident in the asphalt paving or unpaved ground. This is typical of the deformation that we mapped to define the zones shown in Figure 7.1.

Alternate stop: Top of the Hill Road

With more time than is available on this trip, one may see an example of ground deformation coincident with a well-exposed fault in bedrock. Take the East Los Gatos exit from Highway 17, proceed east to Los Gatos Boulevard, turn left (north) onto Los Gatos Boulevard, go three blocks to the first stoplight and turn right (east) onto Kennedy Road. Follow Kennedy Road about 2 1/4 miles to the crest of the divide between Los Gatos Creek and Guadalupe Creek. At this point, turn left onto Top of the Hill Road and park.

Bedrock is exposed in the cut on the uphill side of the road. The near (southwest) end of the roadcut is in strongly deformed

A.

B.

Figure 7.3. Photographs of concrete curbs, sidewalks, and gutters broken by the Loma Prieta earthquake. A) Buckled sidewalk in Los Gatos zone, downtown Los Gatos. View is to southeast. B) Broken curb in Blossom Hill zone, in vicinity of Regnart School, Cupertino. C) Broken curb and gutter in Blossom Hill zone, corner of Garden Lane and Oakdale Drive, near Vasona Dam. View is to northwest. D) Buckled curb along Top of the Hill Road (alternate stop 7). View is to northwest. Intersection of Top of the Hill Road and Kennedy Road is behind figure; roadcut at right margin of photo exposes serpentinite (light rock at extreme right), sedimentary rocks (behind rightmost parked car), and the intervening strand of the Berrocal fault.

sandstone and shale, probably of the Franciscan complex, whereas the far end of the roadcut is in deformed serpentinite. Outcrops on the far side of Kennedy Road are basaltic greenstone of the Franciscan complex. Bailey and Everhart (1964) show a strand of the Shannon fault crossing the Los Gatos Creek - Guadalupe Creek divide at Kennedy Road, that is, at the present intersection of Kennedy and Top of the Hill Road.

The fault contact between the sedimentary rocks and serpentinite is a well-exposed zone of more strongly deformed rock. Fresh offset of the bench in the roadcut, as well as freshly broken rock in the bedrock shear zone, indicated movement on this fault during the Loma Prieta earthquake. Directly along strike several meters to the east, northeast-trending curbs on both sides of Top of the Hill Road were deformed. Buckling of the further curb indicated ~4 cm shortening, compatible with N-S shortening and (or) left-lateral slip. The breaks have since been patched but their locations are still evident. Asphalt between the curbs shows little deformation.

C.

D.

Figure 7.3, continued

Acknowledgments

We would like to thank the following for helping to collect and analyze data presented herein, or for assisting the authors in the preparation of this field guide:

J. Bommer, R. Bucknam, K. Budding, M. Cardinali, K. Chang, M. Clark, W. Cole, P. Cowie, S. Donaldson, R. Eis, T. Fumal, J. Harden, D. Harwood, R. Fisher, D. Knifong, R. Jibson, K. Lajoie, J. Lienkaemper, M. Machette, K. Parish, C. Ramseyer, B. Rogers, Z. Reches, M. Rymer, R. V. Sharp, D. Sorg, and P. Wood.

References

Alexander, C. S., 1953, The marine and stream terraces of the Capitola-Watsonville area: University of California Publications in Geology, 40 p.

Anderson, R. S., 1990a, Evolution of the Santa Cruz Mountains by advection of crust past a restraining bend on the San Andreas Fault: EOS, v. 91, n. 8, p. 287

Anderson, R. S., 1990b, Evolution of the Santa Cruz Mountains by advection of crust past a restraining bend on the San Andreas Fault: Science, submitted 1/1990.

Aydin, A. and Page, B. M., 1984, Diverse Pliocene-Quaternary tectonics in a transform environment, San Francisco Bay region, California. Geological Society of America Bulletin, v. 95, p. 1303-1317.

Bailey, E. H., and Everhart, D. L., 1964, Geology and quicksilver deposits of the New Almaden district, Santa Clara County, California: U.S. Geological Survey Professional Paper 360, 206 p.

Brabb,E. E., 1989, Geologic Map of Santa Cruz County, California: U.S. Geological Survey Miscellaneous Investigations Series I-1905.

Bradley, W. C., 1958, Submarine abrasion and wavecut platforms: Geological Society of America Bulletin, v. 69, p. 967-974.

Bradley, W. C. and Griggs, G. B., 1976, Form, genesis and deformation of central California wave cut platforms: Geological Society of America Bulletin, v. 87, p. 433-449.

Bull, W. B., 1986, Inferred uplift ages and uplift rates of global marine terraces near Santa Cruz, California: Geological Society of America Abstracts with Programs.

Chappell, J. M., 1983, A revised sea-level record for the last 300,000 years on Papua New Guinea: Search, v. 14, p. 99-101.

Clark, J.C., 1981, Stratigraphy, paleontology, and geology of the central Santa Cruz mountains, California coast ranges: U.S. Geological Survey Professional Paper 1168, 51 p.

Clark, C. J., and Reitman, J. D., 1973, Oligocene stratigraphy, tectonics, and paleogeography southwest of the San Andreas fault, Santa Cruz Mountains and Gabilan Range, California Coast Ranges: U.S. Geological Survey Professional Paper 783, 18 p.

Clark, J. C., Brabb, E. E., and McLaughlin, R. J., 1989, Geologic map and structure sections of the Laurel 7 1/2' Quadrangle, Santa Clara and Santa Cruz counties, California: U. S. Geological Survey Open-File Report 89-676, scale 1:24000.

Coppersmith, K. J., 1979, Activity assessment of the Zayante-Vergeles fault, central San Andreas fault system, California: University of California at Santa Cruz Doctoral Dissertation, 216 p.

Cotton, W. R., Fowler, W. L., and VanVelsor, J. E., 1990, Coseismic bedding-plane faulting associated with the Loma Prieta earthquake of October 17, 1989: EOS, v. 91, n. 8, p. 287.

Cummings, J. C., 1968, The Santa Clara Formation and possible post-Pliocene slip on the San Andreas fault in central California, in Dickinson, W.R., and Grantz, A., editors, Proceedings of the conference on geologic problems of the San Andreas fault system: Stanford University Publications in Geological Science, v. 11, p. 191-207.

Dibblee, T. W., and Brabb, E. E., 1978, Preliminary geologic maps of the Chittenden, Los Gatos, and Watsonville East quadrangles, California: U. S. Geological Survey Open-File Report 78-453, 3 sheets, scale 1:24000.

Dibblee, T.W. Jr., 1966, Geology of the Palo Alto quadrangle, Santa Clara and San Mateo Counties, California: California Division of Mines and Geology map sheet 8, scale 1:62,500.

Dietz, L. D., and Ellsworth, W. L., 1990, The October 17, 1989 Loma Prieta, California earthquake and its aftershocks, geometry of the sequence from high-resolution locations: Geophysical Research Letters, in press.

Hall, N. T., 1984, Holocene history of the San Andreas Fault between Crystal Springs Reservoir and San Andreas Dam, San Mateo County, California: Bulletin of the Seismological. Society of America, v. 74, p. 281-299.

Hanks, T. C., Bucknam, R. C., Lajoie, K. R. and Wallace, R. E., 1984, Modification of wave-cut and faulting-controlled landforms: Journal of Geophysical Research, v. 89, p. 5771-5790.

Kennedy, G. L., Lajoie, K. R., and Wehmiller, J. F., 1982, Aminostratigraphy and faunal correlations of late Quaternary marine terraces, Pacific coast, U.S.A.: Nature, v. 299, p. 545-547.

Lajoie, K.R., 1986, Coastal tectonics, in Studies in Geophysics: Active Tectonics: National Academy of Sciences Press, Washington D.C., p.95-124.

Lajoie, K. R., Weber, G. E., Mathieson, S. A. and Wallace, J., 1979, Quaternary tectonics of coastal Santa Cruz and San Mateo countries, California, as indicated by deformed marine terraces and alluvial deposits, in G. E. Weber, K. R. Lajoie and G. B. Griggs, editors, Coastal Tectonics and Coastal geologic hazards in Santa Cruz and San Mateo Counties, California, Geological Society of America Field trip guidebook.

Lawson, A.C., and others, 1908, The California earthquake of April 18, 1906, Report of the State Earthquake Investigations Commission: Carnegie Institute of Washington Publication 87, v. 1, 451 p.

Lisowski, M., Prescott, W. H., Savage, J. C., and Svarc, J. L., in press, A possible geodetic anomaly observed prior to the Loma Prieta, California Earthquake: Geophysical Research Letters.

McLaughlin, R. J., 1974, The Sargent-Berrocal fault zone and its relation to the San Andreas fault system in the southern San Francisco Bay region and Santa Clara Valley, California: U.S. Geological Survey Journal of Research, v. 2, p. 593-598.

References (cont.)

McLaughlin, R. J., 1971, Geologic map of the Sargent fault zone in the vicinity of Mt. Madonna, Santa Clara County: San Francisco Bay Region Environmental and Resources Planning Study, Basic Data Contribution 13, scale 1:12000, 2 sheets.

McLaughlin, R. J., Clark, J. C., and Brabb, E.E., 1988, Geologic map and structure sections of the Loma Prieta 7 1/2' quadrangle, Santa Clara and Santa Cruz Counties, California: U.S. Geological. Survey Open File Map 88-752.

McNally, K. C., Lay, T., Protti-Quesada, M., Valensise, G., Orange, D., and Anderson, R.S., 1989, Santa Cruz Mountains (Loma Prieta) Earthquake: EOS, v. 70, p. 1463,1467.

Merritts, D., and Bull, W. B., 1989, Interpreting Quaternary uplift rates at the Mendocino triple junction, northern California, from uplifted marine terraces: Geology, v. 17: p. 1020-1024.

Nishenko, S. P., and Williams, P. L., 1985, Seismic hazard estimates for the San Jose-San Juan segment of the San Andreas fault: USGS Open file Report 85-0754, p. 1985-2005.

Plafker, G., and Galloway, J. P., 1989, Lessons learned from the Loma Prieta, California, earthquake of October 17, 1989: U. S. Geological Survey Circular 1045, 48 p.

Prescott, W.H., Lisowski, M, and Savage, J.C., 1981, Geodetic measurement of crustal deformation in the San Andreas, Hayward, and Calaveras faults near San Francisco, California; Journal of Geophysical Research, v. 86, n. 10, p. 853-969.

Rode, Karl, 1930, Geomorphogenie des Ben Lomond (Kalifornien), eine Studie uber Terraseenbildung durch marine Abrasion: Zeitschrift fur Geomorphologie, v. 5, p. 16-78.

Sarna-Wojcicki, A. M., Pampeyan, E. H., and Hall, N. T., 1975, Map showing recently active breaks along the San Andreas fault between the central Santa Cruz Mountains and the northern Gabilan Range, California: U.S. Geological Survey Map MF-650, Scale 1:24000.

Scholz, C. H., 1985, The Black Mountain asperity: seismic hazard of the southern San Francisco peninsula, California: Geophysical Research Letters, v. 7, p. 279-282.

Schwartz, D. P. and Coppersmith, K. J., 1984, Fault behavior and characteristic earthquakes: Examples from the Wasatch and San Andreas fault zones: Journal of Geophysical Research, v. 89, p. 5681-5698.

Schwartz, S. Y., Orange, D. L. and Anderson, R. S., Complex fault interactions in a restraining bend on the San Andreas Fault, Southern Santa Cruz Mountains, California: Geophysical Research Letters, submitted 2/1990.

Sorg, D. H., and McLaughlin, R. J., 1975, Geologic map of the Sargent-Berrocal Fault zone between Los Gatos and Los Altos Hills, Santa Clara County, California: U.S. Geological Survey Miscellaneous Field Studies Map MF-643, scale 1:24,000.

Thatcher, W., and Lisowski, M., 1987, Long-term seismic potential of the San Andreas fault southeast of San Francisco: Journal of Geophysical Research, v. 92, p. 4771-4784.

Toppazada, T. R., Reel, C. R., and Park, D. L., 1981, Preparation of isoseismal maps and summaries of reported effects for pre-1890 California earthquakes: California Division of Mines and Geology Open-File Report 81-11, Sacramento, California, 182 p.

Weber, G. E., 1990a, An introduction to marine terraces. in G. E. Weber and G. B. Griggs, Field trip guide for San Francisco Section of the Association of Engineering Geologists, "Coastal geologic hazards and coastal tectonics, northern Monterey Bay and Santa Cruz/San Mateo county coastlines"

Weber, G. E., 1990b, Pleistocene marine terraces and neotectonics of the San Gregorio fault zone, in G.E. Weber and G. B. Griggs, Field trip guide for San Francisco Section of the Association of Engineering Geologists, "Coastal geologic hazards and coastal tectonics, northern Monterey Bay and Santa Cruz/San Mateo county coastlines"

Weber, G. E., Lajoie, K. R., and Griggs, G. B., 1979, Coastal tectonics and coastal geologic hazards in Santa Cruz and San Mateo Counties, California: Field trip guide. Cordilleran section of the Geological Society of America 75th annual meeting.

U. S. Geological Survey Staff, 1990a, The Loma Prieta, California Earthquake: An anticipated event: Science, v. 247, p. 286-293.

U. S. Geological Survey Staff, 1990b, Apparent lithologic and structural control of surface fracturing during the Loma Prieta earthquake of October 17, 1989: EOS, v. 91, n. 8, p. 290.

U. S. Geological Survey Staff, 1989, Preliminary map of fractures formed in the Summit Road – Skyland Ridge area during the Loma Prieta, California, earthquake of October 17, 1989: U. S. Geological Survey Open-File Report 89-686, scale 1:12000.

Yeats, R. S., 1986, Active faults related to folding, in Studies in Geophysics: Active Tectonics: National Academy of Sciences Press, Washington D.C., p. 63-79.